Annu. Rev. Phys. Chem. 2006. 57:65–103
doi: 10.1146/annurev.physchem.57.032905.104748

4D ULTRAFAST ELECTRON DIFFRACTION, CRYSTALLOGRAPHY, AND MICROSCOPY

Ahmed H. Zewail
Laboratory for Molecular Sciences and Physical Biology Center for Ultrafast Science and Technology, California Institute of Technology, Pasadena, California 91125; email: zewail@caltech.edu

Key Words structural dynamics, ultrafast science, molecular imaging, biological imaging

■ **Abstract** In this review, we highlight the progress made in the development of 4D ultrafast electron diffraction (UED), crystallography (UEC), and microscopy (UEM) with a focus on concepts, methodologies, and prototypical applications. The joint atomic-scale resolutions in space and time, and sensitivity reached, make it possible to determine complex transient structures and assemblies in different phases. These applications include studies of isolated chemical reactions (molecular beams), interfaces, surfaces and nanocrystals, self-assembly, and 2D crystalline fatty-acid bilayers. In 4D UEM, we are now able, using timed, single-electron packets, to image nano-to-micro scale structures of materials and biological cells. Future applications of these methods are foreseen across areas of physics, chemistry, and biology.

INTRODUCTION

Chemical and biological structures transform on different timescales through intermediate and transition states on complex energy landscapes, the surfaces of free energy (1). The global shape in nuclear-coordinate space reflects the possible conformations (entropy) and multitude of interactions (enthalpy) that could lead to the change. Over a century of developments (Figure 1), it has become possible in the past two decades to observe the atomic motions (femtochemistry) on their femtosecond timescale (2 and references therein), the scale of vibrational periods. Observed coherent nuclear motions on such timescales define a fundamental transition, from ensemble-rate kinetics to single-molecule-trajectory dynamics.

However, when the systems (molecules or assemblies of them) are those with hundreds or thousands of atoms and the changes involve many possible conformations, one must not only resolve the temporal behavior but also determine the 3D molecular structures during the change. Such combined atomic-scale resolutions in space and time constitute the basis for a new field of study in what we referred to

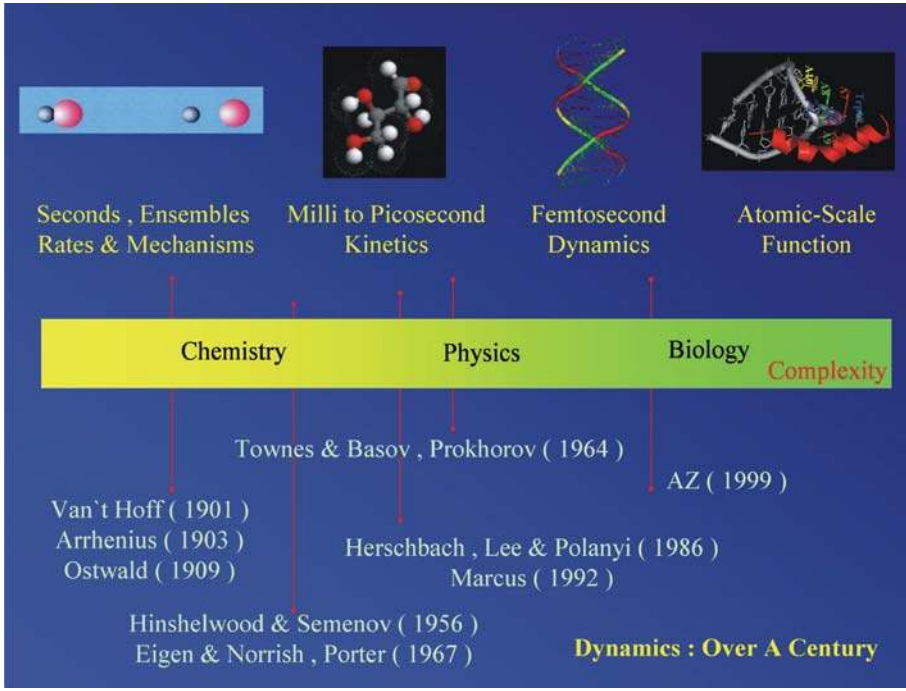

Figure 1 Developments in studies of kinetics and dynamics, from seconds to the femtosecond atomic scale as cited (date indicated) by Nobel prizes over a century.

earlier (see 3; 4 and references therein) as 4D ultrafast electron diffraction (UED), ultrafast electron crystallography (UEC), and ultrafast electron microscopy (UEM; vide infra).

Beginning with the discovery of X rays near the turn of the twentieth century (1895), diffraction techniques have allowed determination of equilibrium (time-averaged) 3D structures, from diatomic salts (NaCl) to DNA, to proteins, and to complex assemblies such as viruses (Figure 2) (5). Of equal importance, after the discovery of the electron in 1897, was the development of electron diffraction for gas-phase structural determination, surface structural analysis, and structural determination of biological systems (Figure 2). In fact the first membrane protein (water insoluble) crystal structure of bacteriorhodopsin (crystal thickness of $\sim$10 nm) was determined using electron diffraction/microscopy (6); determination of the structure of the photosynthetic reaction center, a membrane protein, by X-ray diffraction techniques was achieved in 1985 (7), and more recently the structure of ion channels was successfully completed (8). From the 3D structures determined by electron or X-ray diffraction, one pictures the static spatial arrangements of atoms, but the mechanism for the function cannot be directly unraveled without knowledge of structural dynamics.

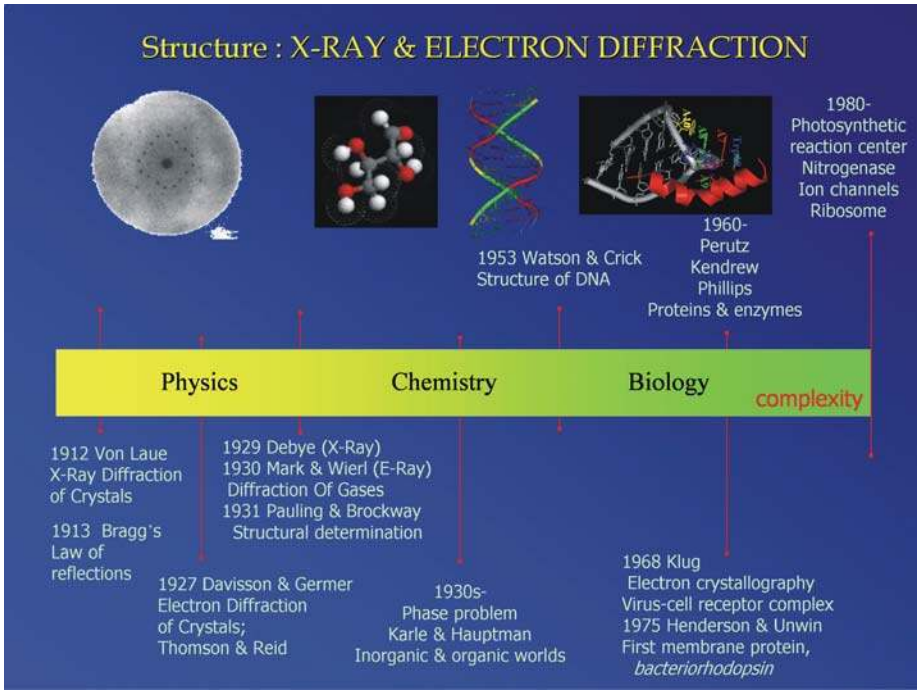

Figure 2 Developments in structural determination, from sodium chloride crystals to DNA and proteins, including the Nobel prizes awarded (date given is that of development).

In our laboratory at Caltech, the methods of choice for structural dynamics have been UED, UEC, and UEM, for the following reasons. First, the experiments are of "tabletop" scale and can be implemented with ultrafast (femtosecond and picosecond) laser sources. Second, the cross-section for electron scattering is about six orders of magnitude larger than that of X-ray scattering. Third, electrons, because of their strong interaction with matter, can reveal transient structures of gases, surfaces, and (thin) crystals. Fourth, electrons are less damaging to specimens per useful elastic scattering event (9). Fifth, electrons can be focused to obtain images in microscopy. And sixth, with properly timed sequences of electron pulses—frame referencing—we are able to "isolate" in time the evolving transient structure(s), as shown below.

In this review, we highlight recent developments of 4D UED, UEC, and UEM at Caltech. We present the methodology for the determination of transient, complex molecular structures (assemblies) with joint spatial (picometer) and temporal (picosecond and femtosecond) resolutions. Examples for applications in different phases are given, including studies of isolated chemical reactions (molecular beams), interfaces, surfaces and nanocrystals, self-assembled monolayers, and 2D crystalline fatty-acid bilayers. We conclude by summarizing the progress made

so far in the direct imaging, in space and time, of nano-to-micro scale materials structures and of biological cells and the potential for exploration in areas of physics, chemistry, and biology. First, however, we will briefly attempt to illuminate the issue of complexity in structural changes and the need for 4D structural dynamics.

COMPLEXITY: WHY 4D?

Even for chemical reactions involving tens of atoms, until recently the determination of intermediate structures in 3D space was impossible because of their fleeting nature on the timescale of a picosecond or less. These transient structures are "dark" in that they undergo radiationless transitions into reactive or nonreactive channels. This bifurcation obscures the mechanism, and only structural dynamical studies can resolve the complexity of pathways and the structures involved, as illustrated below.

Macromolecular structures, with hundreds to thousands of atoms, have the additional complexity of changes involving numerous possible conformations, and with some that are "active" and others "inactive" in the biological function. Such nonequilibrium structures on a complex energy landscape, if determined, can provide an understanding of the origin of reduced-coordinate space for the motion and the real enthalpic and entropic contribution to the free energy. Prime examples of these energy landscapes are those describing protein folding and molecular recognition. Remarkably, the nature and complexity of the transformation are controlled by the balance of weak forces, such as hydrogen bonding, electrostatic interactions, dispersion, and hydrophobic forces, all having energy on the order of a few kcal/mol.

It is perhaps useful to consider cases where the function and dynamics are strongly correlated. In our laboratory, we have studied the dynamics of the elementary processes involved in molecular recognition, protein hydration, and electron transfer (Figure 3). The timescales were directly established, but the transient structures at the critical stage of the function remained unknown. For example, the recognition of myoglobin to dioxygen, and similarly of a model picket fence to dioxygen (Figure 3), were studied on the femtosecond and up to the millisecond timescale. We were able to obtain the timescales for oxygen liberation, rebinding, and escape from the macromolecular structure. We also measured the diffusion-controlled rates (k_{on}) and the dissociation rates (k_{off}) of the complexes. From the results, we inferred the global nature of the landscape (10–12). But we still know little about the active intermediate structure(s) critical to the different pathways in the protein. These structures cannot be optically resolved.

Similarly, for RNA recognition of proteins (Figure 3), the dynamics of the complex was found to be interfacial and is controlled by a single residue, the interface between tryptophan of polypeptides and bases of RNA (13, 14). The recognition is critically dependent on conformational structures, stacked (active) or unstacked

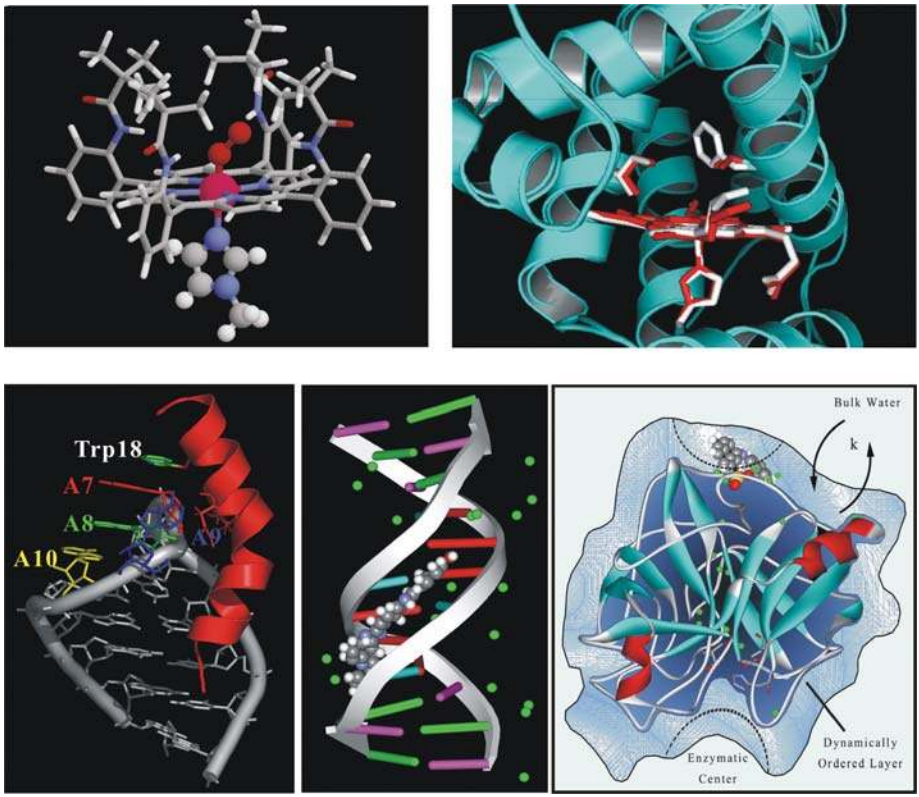

Figure 3 Biological structures studied for their role in molecular recognition, charge transport, and hydration. From top left: picket fence mimic of myglobin, myglobin, RNA-polypeptide complex, DNA-drug complex, and protein (α-chymotrypsin) hydrated by a dynamically ordered water layer (see text).

(inactive). The in vivo function (antitermination) experiments showed strong correlation with the femtosecond dynamics. The femtosecond timescale is unique to the active structures; the inactive structures have a nanosecond timescale. We do not know the precursor transient structures and the extent of conformational flexibility.

The final examples given here are those of the DNA structures involved in electron transport and protein structures involved in interfacial water hydration (Figure 3). The "mobility" of electron transport in DNA duplexes was found to be essentially controlled by the dynamics of stacked structures on the timescale of the transport (15 and references therein; 16). Protein structures in water were found to be dynamically hydrating (on the picosecond timescale) for them to reach the folded state, and hydration plays a significant role in the function (17 and references therein; 18). Neither structures were determined during the act.

From these representative studies it is clear that for such complex structures, with complex free energy landscapes, an understanding of the function requires an integration of the trilogy:

Structure—Dynamics—Function.

Though time-averaged molecular structural determination is important, the static structures do not elucidate the nonequilibrium functional structures, and 4D determination in space and time can uncover the true nature of the landscape.

Before highlighting three related developments at Caltech, it is important to realize two concepts involved in structural dynamics—the time-energy uncertainty and the relevant timescales. First, there should be no concern about the uncertainty principle in limiting the information to be gained from femtosecond-to-picosecond time resolution, as all structures are prepared coherently (2 and references therein; 19, 20). Second, for any dynamical process, the change with time is continuous, and although some global events may occur at longer times—so-called "relevant timescales"—these events are triggered by changes at early times. The primary events are an essential part of any complete description of the landscape and the dynamics. Thus the notion that "relevant" biological events occur only far beyond the ultrafast time domain gives an incomplete picture and may prove, as in early notions of chemical reactions (2), to be inaccurate.

EVOLUTIONS AND REVOLUTIONS

As in the evolution (revolution) of any field, tools and concepts have been equally important in the developments of UED, UEC, and UEM. For studies with electrons, Young's interference (1801), J.J. Thomson's corpuscle (1897), de Broglie's postulate of the electron's wave nature (1924; Doctoral Thesis), and Debye's work on diffraction and structure of gases (1915, 1929) provided the foundation. Gas phase electron diffraction (GED) was observed first by Mark & Wierl in 1930 (21), only three years after the discovery of electron diffraction by Davisson & Germer for a crystal of nickel (22) and by G.P. Thomson (the son of J.J.) & Reid for thin films of aluminum, celluloid, and other materials (23). Methods and applications have progressed over the following decades, culminating in studies of (time-averaged) structures that were—since Pauling's days—and still are important for the understanding of the nature of the chemical bond (see, e.g., 24; 25 and references therein). Thousands of static structures were obtained using GED. For solids, progress has been made in many areas of studies (26 and references therein), including those of low-energy electron diffraction (LEED) and reflection high-energy electron diffraction (RHEED). For biological studies, as mentioned above, microscopy and diffraction are powerful tools in structural determination.

Determining transient molecular structures on the ultrafast timescale demands not only the marriage of ultrafast probing techniques with those of conventional

diffraction, but also the development of new concepts for reaching simultaneously the temporal and spatial resolutions of atomic scale. Progress has been made in advancing X-ray diffraction and absorption methods [e.g., see 27 (and references therein), 28–33 and below] but here we focus on the developments involving ultrafast electrons in UED, UEC, and UEM, for reasons discussed below.

Following the development of femtochemistry in the mid-1980s, we embarked upon a new challenge, that of achieving time-resolved ultrafast electron diffraction for structural determination. In 1991, we proposed that replacing the "spectroscopic probes" of femtochemistry with ultrashort electron pulses would open up a new field for studying the nature of transient structures and their coherent atomic motions (34, 35). A year later, we reported diffraction patterns with picosecond electron pulses ($\sim$10 ps), but without recording the temporal evolution of the reaction in the gas phase (36). Since those first images, the technical and theoretical machinery had to be developed, evolving from the first-generation apparatus (UED-1) (36) to the second (UED-2) (37), and culminating in the third-generation apparatus (UED-3). In UED-3, the spatial and temporal resolutions are 0.01 Å and 1 ps, respectively (38), for isolated molecular beams studies, and the sensitivity of detecting a chemical change is as low as 1%. We then constructed UED-4 for the sole purpose of UEC (39, 40) in reflection and transmission modes and reached in this apparatus the atomic-scale spatial (picometer) resolution and the femtosecond time (300-fs) resolution, as discussed below; Figure 4 portrays the apparatus schematic for both UED and UEC. In 2004, we embarked on the development (3 and references therein; 41) of UEM (Figure 5), with capabilities for single-electron, femtosecond ($\leq$100 fs) diffraction (UED-5), and microscopy.

For UED and UEC, the leap forward came from the integration of new 2D digital processing with CCD cameras, the generation of ultrashort electron packets using femtosecond lasers and high extraction fields, and the in situ pulse sequencing and clocking (4 and references therein)—all of which gave us unprecedented levels of sensitivity and spatiotemporal resolution to perform real experiments. Perhaps the most critical advance was the development of the frame-reference method; earlier we termed it the diffraction-difference method (4 and references therein; 42), but because of the development of UEC and UEM we find referring to it as the frame-reference method to be more general. When properly timed frame referencing is made, before and during the change, the evolving transient structures can be determined. Armed with these developments, we have studied a variety of complex molecular structures, resolved their temporal evolution, and studied phenomena both in the gas and condensed phases and on surfaces, as discussed below. For UEM, the paradigm shift, after many failed attempts to reach space-charge-free focusing and temporal broadening, was the development of timed, single-electron packets for imaging of materials structures and biological cells.

The earliest efforts at introducing time resolution into electron diffraction were not developed for the ultrashort time domain. As in flash photolysis (2 and references therein), studies of radicals with electron diffraction were made using

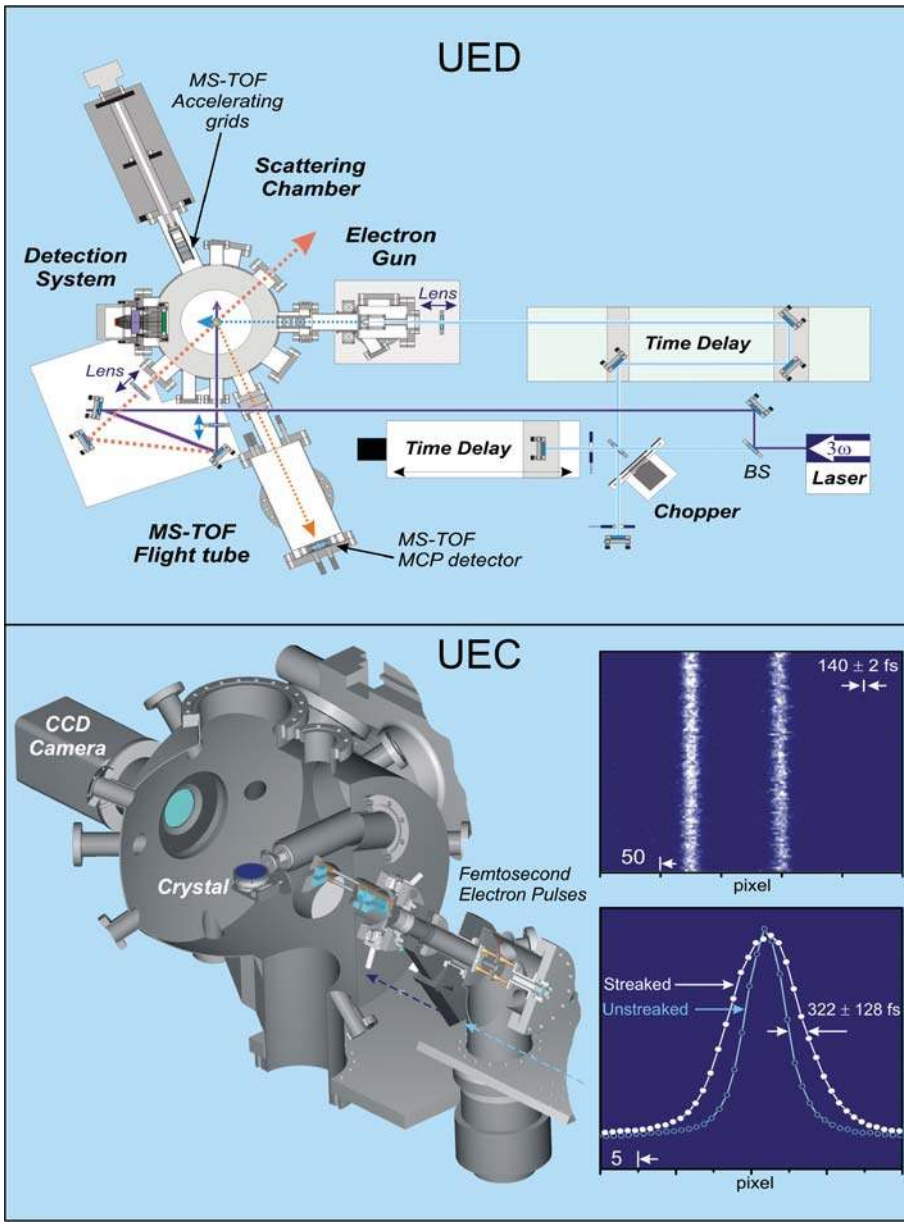

Figure 4 Schematic of ultrafast electron diffraction and ultrafast electron crystallography apparatus, together with the in situ measured electron pulse streaks and width (see text for details).

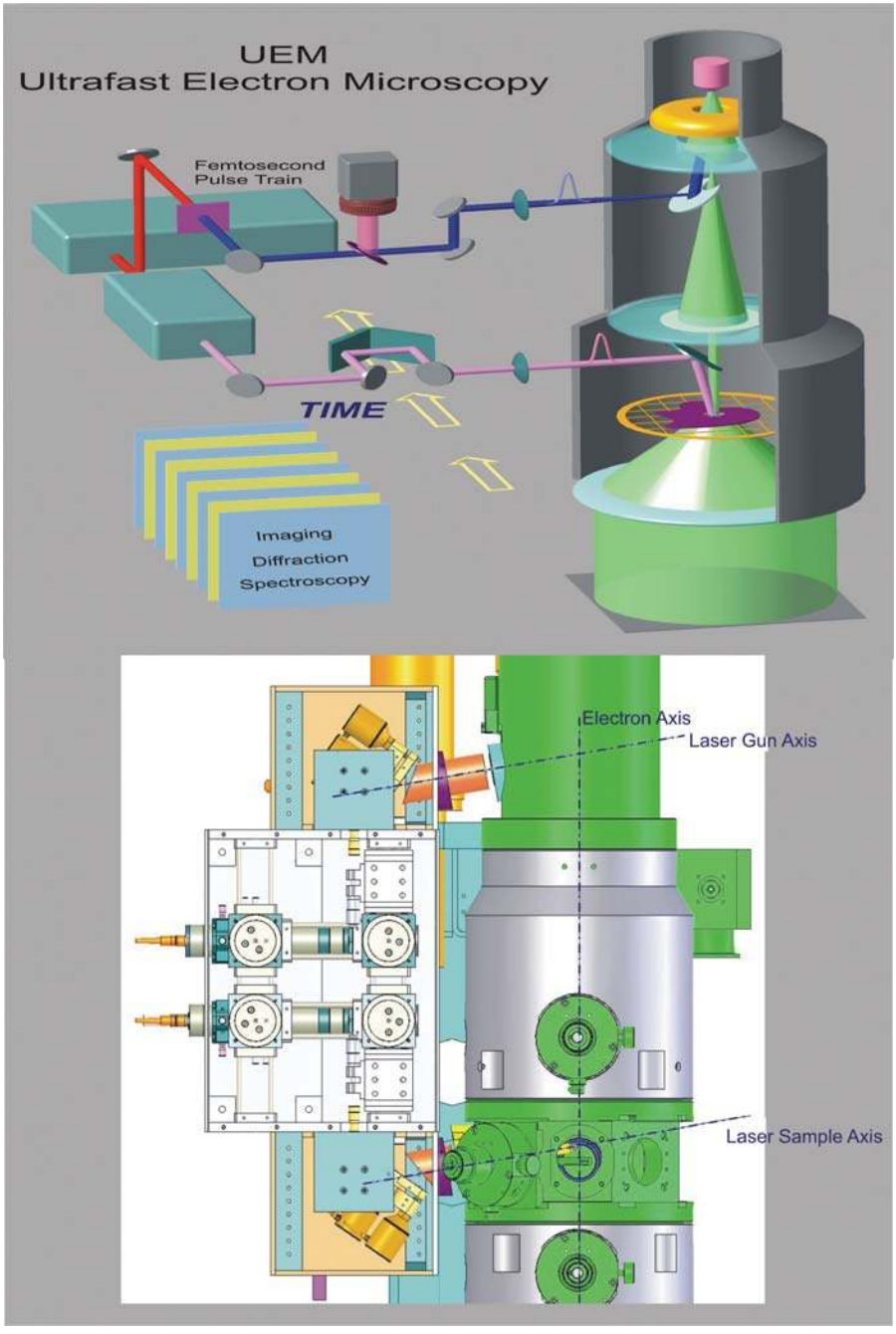

Figure 5 Schematic of ultrafast electron microscopy apparatus, and a close-up of the design for femtosecond pulse interface to the microscope.

electronic circuitry ("shutters") on the milli-to-micro second timescale. The patterns, if properly deconvoluted from the contribution of the precursor, only give the structure of the radical, not its molecular history or the reaction dynamics. As such, studies of this type provide valuable information on the structures of radicals (stable or metastable), but both the approach and time resolutions are inadequate for obtaining direct information of the dynamics on the ultrashort timescale.

With submillisecond recording, Rood & Milledge (43) conducted studies of the radical $ClO^{\bullet}$, from ClO_2, by combining flash photolysis and gas-phase electron diffraction. A year earlier, using a different apparatus, Ischenko et al. (44) reported on studies of infrared multiphoton excitation of CF_3I, but the time resolution of the processes involved was not provided; for a critique, see References 43 and 45. Bartell & Dibble (46) studied phase change in clusters produced in supersonic jets, with a time-of-flight resolution of ca. 1 μs. Ewbank et al. (47, 48) advanced the temporal resolution to nanoseconds (and later into the subns) by combining an intense-laser initiated electron source with a linear diode array detector, operating in the space-charge limit ($\sim 10^{10}$ electrons per pulse). The groups of Schäfer and Ewbank made careful investigation of the photofragments of small molecules (e.g., CS_2) and their internal energies. Recently, Weber's group (49) has succeeded in obtaining UED patterns, that of cyclohexadiene in the gas phase, a system we have studied both theoretically and experimentally, as referenced below.

In 1982, Mourou & Williamson (50) introduced the methodology of a modified Bradley-Sibbett streak camera to record diffraction from thin aluminum films in a transmission mode with 100-ps pulses; subsequently, 20-ps electron pulses were produced to study the films before and after irradiation with a laser (51). Elsayed-Ali and colleagues succeeded in using 200-ps (and later shorter) electron pulses to investigate surface melting with RHEED (52, 53). More recently, the groups of Cao (54) and Miller (55) have focused their efforts on the shortening of the pulses (vide infra) and demonstrations also on solid films of aluminum. For microscopy, the developments are more recent and will be covered in the section on UEM.

ULTRAFAST ELECTRON DIFFRACTION

The Frame-Reference Method and Clocking of Structures

The UED technique employs properly timed sequences of ultrafast pulses—a laser pulse to initiate the reaction and an electron pulse to probe the ensuing structural change in the molecular sample (Figure 6). The resulting electron diffraction patterns are then recorded on a CCD camera. This sequence of pulses is repeated, timing the electron pulse to arrive before or after the laser pulse; in effect, a series of snapshots of the evolving molecular structure are taken in a continuous recording. Each time-resolved diffraction pattern can then, in principle, be inverted to reveal the 3D molecular structure that gave rise to the pattern at that specific time delay.

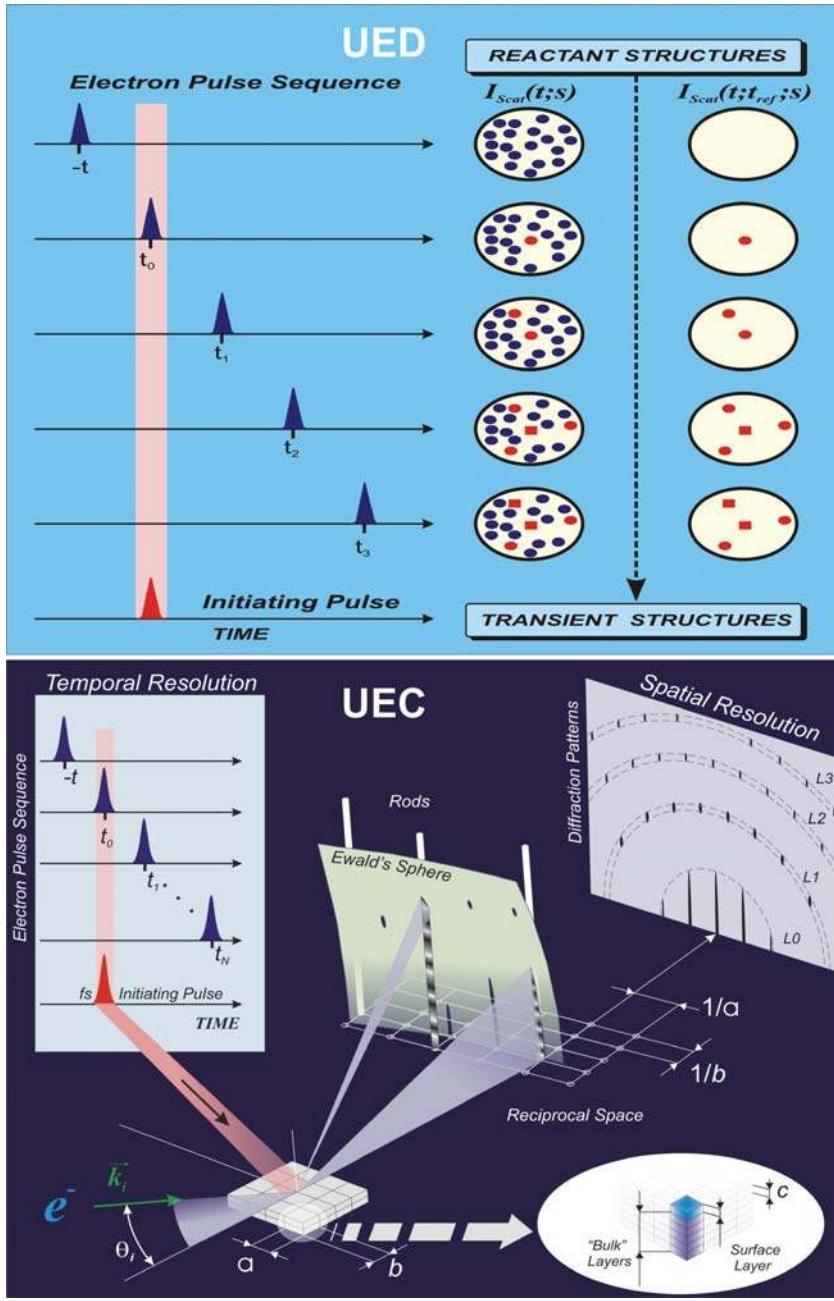

Figure 6 (*Top*) Concept of ultrafast electron diffraction. (*Bottom*) Concept of ultrafast electron crystallography. Note the progressive frame referencing that can be made at different times. The Laue zones are denoted by *L* in the reciprocal space.

However, in practice, a key challenge lies in recovering the molecular structural information that is embedded in the as-acquired diffraction images.

One of the most powerful features of electron diffraction is that the electrons scatter off all atoms and atom-atom pairs in the molecular sample. Thus, unlike spectroscopy wherein the probe is tuned to specific transitions, the electron probe is sensitive to all species in its path and can hence uncover structures that spectroscopy may be blind to. However, it is this strength of UED that also poses a tremendous challenge in retrieving information on molecular structure change. The recorded electron diffraction patterns contain contributions from incoherent atomic scattering as well as the coherent molecular interferences arising from atom-atom pairs. Because there is no long-range order in gases to enhance coherent interferences, the incoherent atomic scattering from gases is orders of magnitude higher. Also, because the fraction of molecules undergoing change is small (typically 10% or less), the recorded diffraction patterns contain large contributions from unreacted molecules.

A key advance in accessing this small population of changing structures embedded in the large background signal has been the application of the frame-reference method mentioned above. The method consists of timing the electron pulses so as to establish an in situ reference signal, usually the ground-state structure obtained at negative time, or one of the evolving structures at positive times. At different reference times (t_{ref}) we can isolate selective changes, as shown in Figure 7. The nature of our digital processing methodology then allows us to obtain the difference of each time-resolved diffraction pattern from a particular reference signal. The methodology will be demonstrated below for a two-step chemical reaction.

The frame-reference method has several general advantages. First, the large (unwanted) background signal from atomic scattering is a common contribution to all images—regardless of the temporal delay and the nature of the reaction—and can, therefore, be practically eliminated in the difference. Thus, whereas the total diffraction signal is dominated by the background intensity, the frame-reference curve is dominated by the molecular scattering intensity. Second, any intrinsic systematic error of the detection system will effectively be eliminated or greatly reduced by the difference. Third, each frame-reference pattern reflects comparable contributions from the reactant and transient structures—in contrast, in the original raw data, only a relatively small fraction of the signal comes from transient structures, with the vast majority of the signal originating from the unreacted parent. Therefore, the significance of transient structure contribution is dramatically enhanced in the frame-reference patterns.

This development of the frame-reference methodology, combined with the high sensitivity achieved by the design of our CCD detection system, provides the impetus for investigating diverse molecular phenomena with UED. However, several other conceptual challenges had to be surmounted. First, there had not previously been a way to determine in situ the zero-of-time (clocking) in UED experiments. Second, for an ultrafast electron pulse, electron-electron repulsion takes place. These space-charge effects broaden the pulse duration over time, leading to a

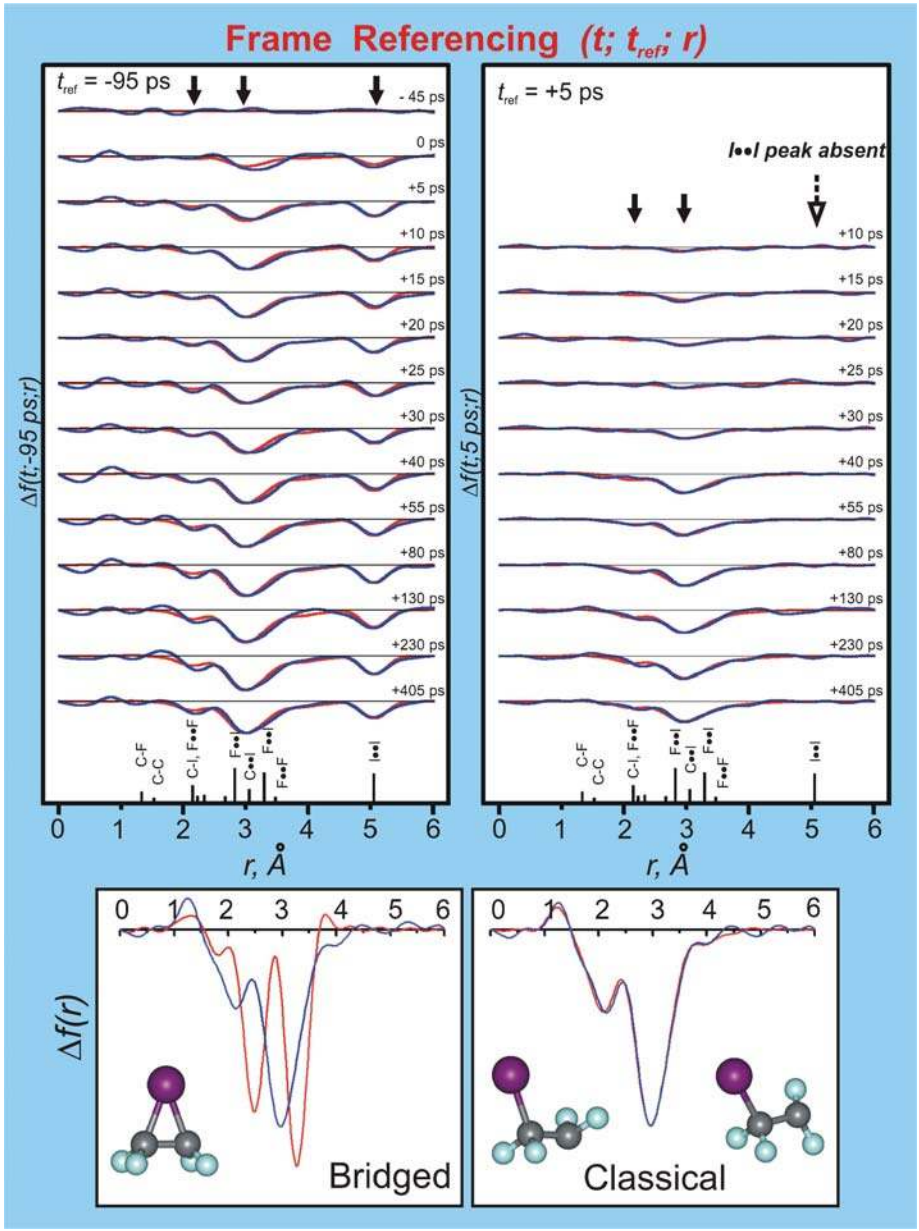

Figure 7 Frame-referencing methodology applied to the determination of structures in the elimination reaction of $C_2F_4I_2$. Note the absence of the peak at ~5 Å as t_{ref} was selected at +5 ps (instead of negative time). The structure of the intermediate is determined to be classical, as evidenced by the agreement between diffraction theory and experiment.

trade-off between temporal resolution and the electron pulse density. Third, the orders-of-magnitude lower density of gas-phase samples relative to solids and surfaces results in much weaker scattering intensities. Last, the limited extent of reaction requires unprecedented sensitivity in the number of molecules detected. These challenges in UED were major hurdles that had to be circumvented in order to reach the current state-of-the-art.

To clock the change on the picosecond/femtosecond timescale, we have developed an ion-induced "lensing method" (56). Basically, in the same diffraction apparatus, we use a laser beam to induce gas ionization through femtosecond multiphoton processes. The generated photoelectrons escape this ionized region and leave behind positively charged ions whose transient electric field in the formed plasma acts as an effective lens and "focuses" the electron beam, only when both the laser and electron pulses temporally overlap. In this way we can identify the zero-of-time, or the threshold, for the purpose of clocking the change.

Finally, to limit space-charge-induced broadening, the electron density in the ultrashort electron packets is maintained low; 1 ps electron pulses typically contain 1000 electrons in the UED apparatus (38). Consequently, the total scattering intensity is considerably lower when compared with conventional GED experiments. The orders-of-magnitude difference in the beam current of UED (pA) relative to conventional GED experiments (μA to mA) must be accounted for by the detector sensitivity and length of the exposure. The introduction of a sensitive CCD camera system capable of single-electron detection was the key to overcoming this problem. For UEC and UEM, we also invoke the frame-reference method, but the incoherent diffraction is much attenuated. As shown below, it is possible to reach the femtosecond timescale because of the increased sensitivity due to this long-range order in UEC and the single-electron imaging in UEM. We give examples of studies in UED below.

Prototype Example: Chemical Reactions

The temporally and spatially resolved transient structures elucidated by UED have now been studied in different reactions for excited states and for conformations at nonequilibrium geometries. A textbook case is that of the nonconcerted elimination reaction of dihaloethanes. It demonstrates the UED methodology of using different electron-pulse sequences to isolate the reactant, intermediates-in-transition, and product structures. The specific reaction studied involves the elimination of two iodine atoms from the reactant (ethanes) to give the product (ethylenes). The structures of all intermediates were unknown, and the challenge lay in determining the structural dynamics of the entire reaction. As detailed elsewhere (57, 58), this was achieved by referencing the diffraction to different time frames (–95 ps and +5 ps); see Figures 7 and 8. The temporal evolution of the two steps of the reaction was also recorded, for the final step as a rise (25 $\pm$ 7 ps), and for the intermediate as a decay (26 $\pm$ 7 ps).

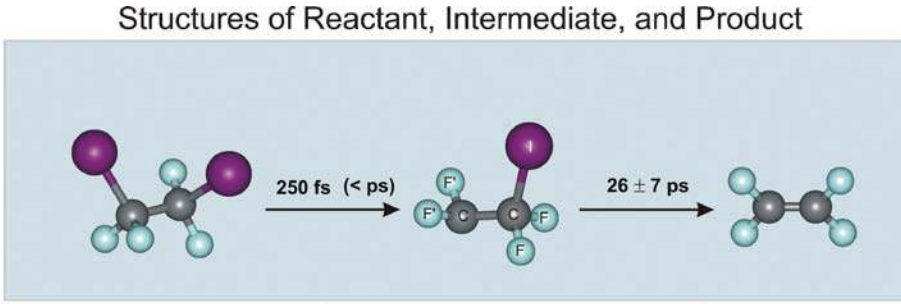

Distances

	experiment	ab initio anti	ab initio gauche
r(C-C)	1.534 ± 0.013	1.532	1.540
r(C-F)	1.328 ± 0.003	1.320	1.323
r(C-I)	2.136 ± 0.007	2.159	2.147

Angles

α (C-C-F)	109.4 ± 1.0	109.0	107.6
α (C-C-I)	111.6 ± 1.0	111.9	114.8
α (F-C-F)	107.8 ± 1.0	108.7	107.9
ϕ^{anti}(IC-CI)	180 (fixed)	180.0	
ϕ^{gauche}(IC-CI)	70 ± 3		67.8

Distances

	Experiment	ab initio anti	ab initio gauche
r(C-C)	1.478 ± 0.049	1.503	1.508
r(C-F)	1.340 ± 0.037	1.322	1.327,1.323
r(C-I)	2.153 ± 0.013	2.164	2.149
r(C-F')	1.277 ± 0.027	1.304	1.309,1.307

Angles

α (C-C-F)	108.6 ± 6.0	108.6	109.8,108.1
α (C-C-I)	115.0 ± 3.1	112.7	111.8
α (F-C-F)	108.0 ± 11.2	108.8	108.0
α (C-C-F')	117.9 ± 3.1	114.0	112.3,113.8
α (F'-C-F')	119.8 ± 7.8	111.8	111.2

Distances

	Experiment	DFT
r(C-C)	1.311 ± 0.021	1.306
r(C-F)	1.319 ± 0.006	1.312

Angles

α (C-C-F)	123.8 ± 0.6	123.8

Figure 8 Structures determined for the reactant, intermediate, and product of the elimination reaction indicated (*top*). The distances and angles are given for the refined structures.

The molecular structure of the C_2F_4I intermediate was determined from the frame referencing curves of ΔsM (t; 5 ps; s). Both the bridged and classical C_2F_4I structures were considered in the analysis of the diffraction data. The theoretical curves for the classical structures reproduce the experimental data very well, whereas the fit provided by the theoretical bridged structure is vastly inferior (Figure 7). Thus, we concluded that the structure of the C_2F_4I radical intermediate is, in fact, classical in nature—the iodine atom does not bridge the two carbons.

The structural parameters of the C_2F_4I intermediate are given in Figure 8. The C–I and C–C distances of the C_2F_4I intermediate are, respectively, longer and shorter than those of the reactant, whereas the C–F′ internuclear distance in the radical site ($–CF'_2$) is shorter than that of the $–CF_2I$ site. These results elucidate the increased C–C and decreased C–I bond order resulting from the formation of the transient C_2F_4I structure. Moreover, the ∠CCF′ and ∠F′CF′ angles become larger than the corresponding angles of the reactant (by ∼9° and ∼12°, respectively), suggesting that the radical center ($–CF'_2$) of the C_2F_4I intermediate relaxes following loss of the first I atom. The structures and dynamics reported for this reaction are vital in describing the retention of stereochemistry in this class of reactions (57, 58), and this is the first example of resolving such complex structures during the transition to final products.

Dark Structures: Bifurcations in Radiationless Transitions

Another example in the applications of UED is that of excited-state structures, bifurcating to undergo radiationless transitions and chemical reactions. For example, in a recent publication (59), four prototypical hetero-aromatic (pyridine, 2-methylpyridine and 2,6-dimethylpyridine) and aromatic-carbonyl (benzaldehyde) organic molecules have been studied. For these molecules and others studied (Table 1), we determined the initial ground-state structure and followed upon excitation the changes in the diffraction pattern with time (Figures 9 and 10). The depletion of old bonds and emergence of new bonds elucidate the structural origin of dark transitions in the hetero-aromatics and the quinoid-like excited-state structure of triplet benzaldehyde. Of significance is the understanding of the influence of parent structure on the dynamical evolution of relaxation pathways and their relative timescales, and the possible bifurcation into physical and chemical channels on the energy landscape.

For the studies of the pyridine series, we focused on the so-called channel three phenomenon, wherein, at a given internal energy threshold, the nonradiative decay rate increases abruptly with concomitant drop in the emission quantum yield. The channel three onset is much more pronounced for pyridine and picoline (2-methlypyridine) than for lutidine (2,6-dimethlypyridine). Two fundamental questions were unanswered: What is the origin of the abrupt change in the radiationless behavior of the pyridines above a certain input energy threshold? Furthermore, how are such radiationless processes influenced by subtle changes in the molecular structure?

On the basis of the determined transient structures, we concluded that upon excitation, pyridine and picoline undergo C–N bond scission to open the aromatic ring and form a diradical structure. Lutidine does not undergo ring opening, but instead gives vibrationally hot ground/electronic state species. The refined structures of ring-opened pyridine and picoline show alternating single- (near 1.45 Å) and double-bond (near 1.35 Å) character for the skeletal distances, indicating disruption of the aromaticity of the parent ring structure. Moreover the farthest $C \cdots N$ distances (reflected as positive contributions in Figure 10) are >4 Å, which are absent in the $f(r)$ of the parent ground-state structure. The refined hot lutidine structure(s) shows the retention of aromatic distances in the product. The populations of these transient structures gave the temporal growth with time constants of 17 ± 1 ps, 28 ± 7 ps, and 16 ± 2 ps, for pyridine, picoline, and lutidine, respectively. The disruption of the ring, or lack thereof, was elucidated in recent calculations of charge density maps by Shorokhov et al. in this laboratory and is fundamentally due to the nature of the $n\pi^*$ versus $\pi\pi^*$ excitation.

Can we determine excited-state structures and their possible bifurcation? The study of the aromatic carbonyl benzaldehyde makes the answer affirmative. Upon light absorption, benzaldehyde undergoes efficient nonradiative intersystem crossing to the triplet state as evidenced by its high phosphorescence yield. Previous investigations revealed photochemical dissociation into benzene and carbon monoxide above an internal energy threshold (~35,000 cm^{-1}). We sought to

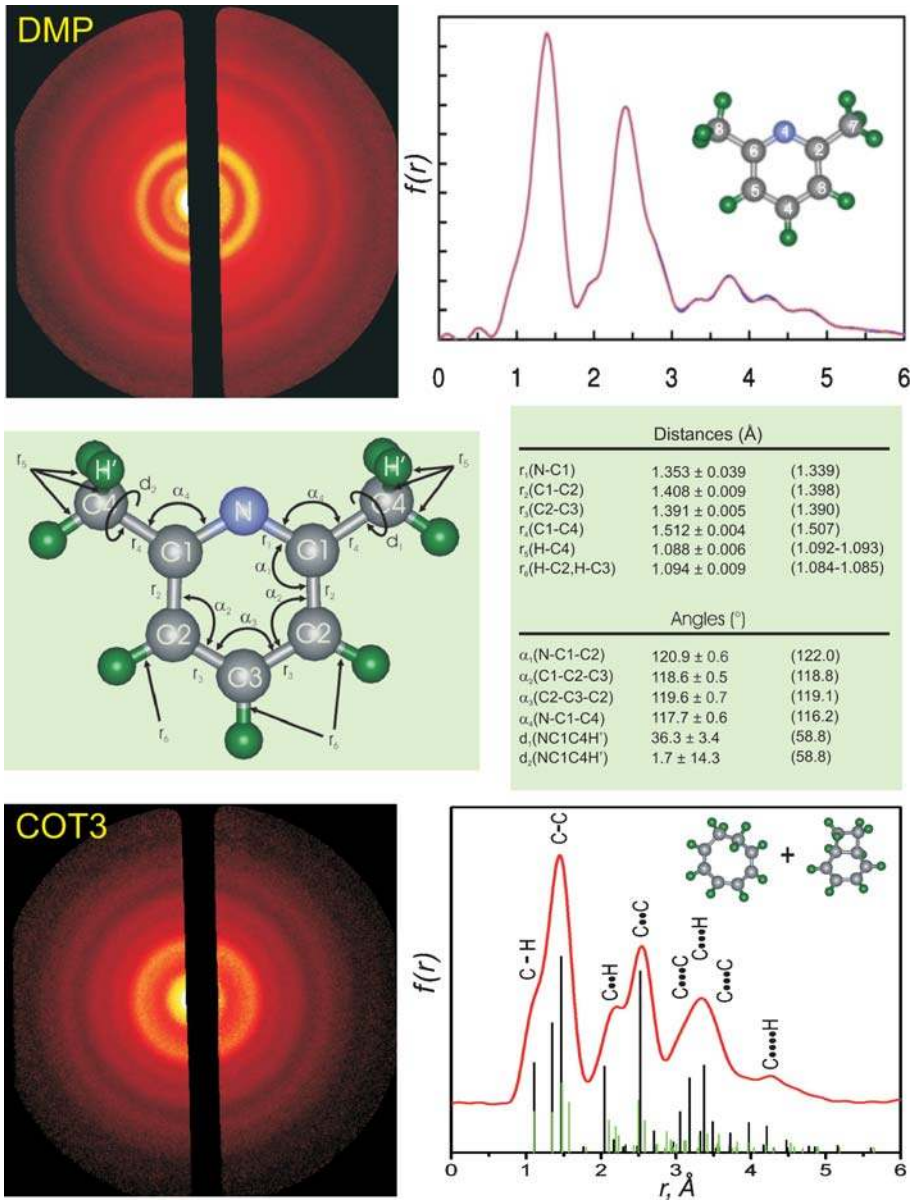

Figure 9 Diffraction images and radial distribution functions *f(r)*, together with structural parameters for the indicated molecules (see text for details). DMP, dimethylpyridine; COT3, cycloocta-1,3,5-triene.

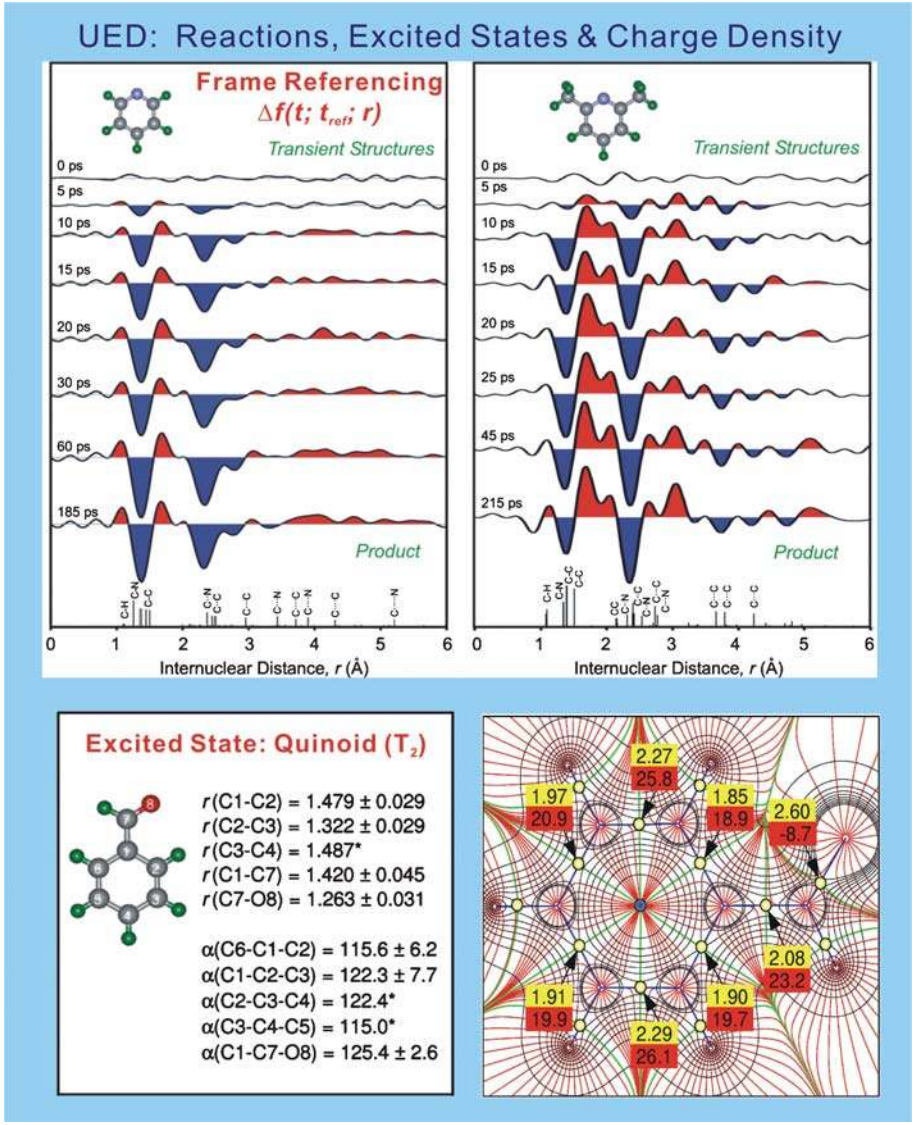

Figure 10 Structural dynamics for two reactive systems (*top*) and for the excited triplet state (quinoid structure) that resulted from radiationless transition of benzaldehyde. The calculated charge density map shows the quinoid structure in agreement with experiment (the calculated image to scale is in Reference 60).

determine the structures and pathways—whether the photophysical and photochemical processes occur consecutively or else competitively as a result of bifurcation. The diffraction data show the rupture of covalent C–C bonds (near 1.4 Å), loss of next-nearest neighbor distances (near 2.5 Å), and depletion of longer distances (>3.5 Å)—a fragmentation and significant repositioning of the atomic nuclei must accompany the process.

We determined a quinoid structure, which is optically dark, for the triplet excited-state ($\pi\pi^*$) benzaldehyde formed as a result of intersystem crossing. This excited-state structure exhibits well-defined single and double bonds, indicating disruption of aromaticity in the ring (Figure 10). On the other hand, benzene formed in the dissociation pathway is in its ground electronic state, as indicated by the refined C–C bond distance. The simultaneous emergence of the photophysical and photochemical products in the diffraction data indicates a bifurcation on the excited singlet surface with apparent rise, through the intermediate, with time constants of 25 $\pm$ 4 ps and 38 $\pm$ 5 ps for excited triplet benzaldehyde and benzene, respectively. This observed bifurcation resolves long-standing issues. The quantum chemical calculations of charge density maps by Shorokhov et al. (60) (Figure 10) support the conclusion regarding the electronic distribution of the structures involved in the bifurcation.

Complex Landscapes and Light-Atom Structures

In order to extend these studies to systems of more complex energy landscapes and to structures with no heavy atoms, we studied organometallic structures, which react through multiple pathways and yield products of different spin multiplicity, and a series of hydrocarbons that undergo thermal/photochemical reactions. We determined the initial structures with high accuracy and those of the reaction intermediate(s). For the hydrocarbons, the sensitivity was still high even though there were no heavy atoms to scatter from. The landscape involves multiple conformations and we studied these nonequilibrium structures, both experimentally and theoretically. More recently, we reported our study of the nature of the hydrogen bond in acetylacetone and the structural dynamics of its elimination reactions. We also concerned ourselves with the theoretical treatment of diffraction on the ultrashort timescale with particular focus on the role of coherence and the effect of orientational order on diffraction of reacting populations. We do not cover these studies in this review, but reference to these and other studies is made in Table 1.

ULTRAFAST ELECTRON CRYSTALLOGRAPHY

In UEC, the new features of the apparatus include three interconnected ultra high vacuum (UHV) chambers—the sample preparation, load-lock, and scattering chambers. To this apparatus we interfaced a femtosecond laser system. The crystal is mounted on a computer-controlled goniometer for high-precision (0.005°) angular rotation; it can be cooled to a temperature of 10 K and changed in five

directions, three translations, and two rotations. The preparation chamber has sputtering and cleaning tools and is also equipped with LEED and Auger spectroscopy for characterization of the crystal surface. Molecules can be studied on the surface either as physisorbed or chemically functionalized entities, and thin crystals can be studied in the reflection mode. We have also used the apparatus in the transmission mode for studies of crystals and thin films.

Diffraction is recorded in the far field and analyzed using the observed Bragg spots, streaks, and Laue zones of Ewald's sphere (Figure 6). The electron and light pulses used in UEC were temporally and spatially characterized. For the 30 keV electron pulses, we used in situ streaking techniques and, for light, the now standard autocorrelation method. We have obtained the fastest streaking speed of 140 ± 2 fs/pixel in UED-4, thus approaching the state of the art in streak cameras (Figure 4). For the extraction field of 10 kV/mm, the spreading time is $\sim$20 fs. From the measured streaking, a pulse width of 322 ± 128 fs was obtained. Using the same electron gun design, Cao et al. (54) obtained $\sim$300 fs pulses, albeit with a streaking speed of 250 fs/pixel. Miller's group reported $\sim$600 fs resolution in transmission (55). The initiation laser pulse duration is typically 100 fs, and the overall temporal resolution is determined by the geometry of the experiment and the relative widths (shapes) and speeds of the two pulses. We have treated in detail elsewhere (61) conditions for velocity mismatch and its angular dependence for optimum pulse width. In what follows we give examples of studies in UEC.

Surfaces and Crystals

A paradigm case study demonstrating the potential of UEC was reported by Vigliotti et al. (62). Determination of surface structural dynamics, using frame referencing, was achieved for crystalline solids (GaAs), following the temperature rise of the crystal. From the change of Bragg diffraction (shift, width, and intensity), we showed by direct inversion of the diffraction data that "compression" and "expansion" occur on the –0.01 Å to +0.02 Å scale, and that the "transient temperature" reaches its maximum value (1565 K) in 7 ps (Figure 11). The onset of structural change lags behind the rise in the temperature, demonstrating the evolution of nonequilibrium structures. These results were compared with those of nonthermal femtosecond optical probing reported by Mazur's group (63), and the agreement for the temperature response from the fluence dependence of the dielectric function is impressive, but we now have the dynamical structure.

The surface of GaAs was functionalized with a monolayer of chlorine atoms, chemically bonded. On the ultrashort timescale we observed, following the compression, the expansion that is due to the rise of phonon temperature. At longer time, the restructuring and the evolution toward the equilibrium state was clearly evident in the diffraction (intensity and shift). Structural dynamics can be divided into three regimes: potential driven change, which involves electronic redistribution with no motion of nuclei (femtoseconds to a few picoseconds); coherent nonequilibrium lattice expansion (rise time of 7 ps); and restructuring and heat diffusion (50 ps to nanoseconds). The latter agrees well with the expansion reported in the literature

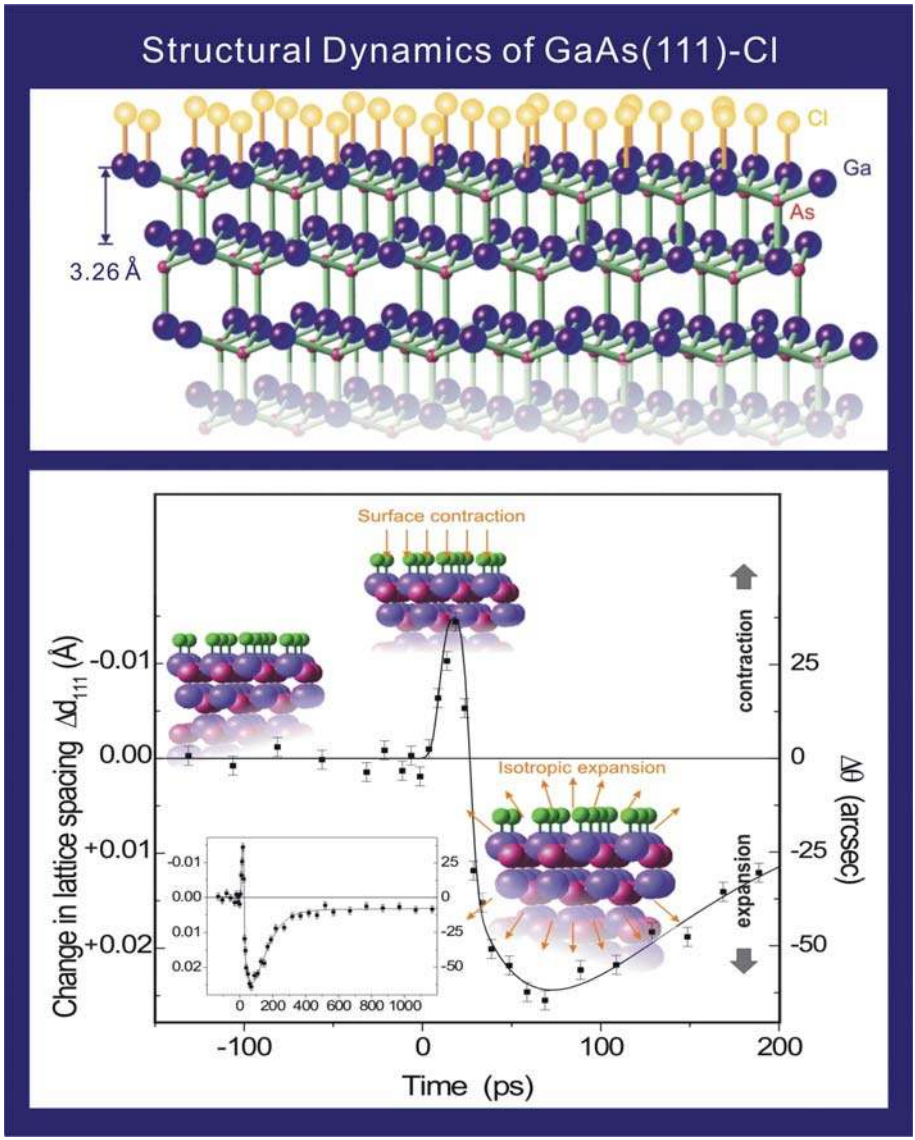

Figure 11 Ultrafast electron crystallography studies of GaAs single-crystal surfaces, terminated with chlorine atoms. Shown here is only the change (from equilibrium) of the lattice constant. The broadening and intensity of diffraction peaks were also monitored, and studies of this system are continuing in this laboratory (see text).

for thermal heating ("infinite" time limit). We are continuing studies of this system because of, among other findings, the discovery of changes in signal phase when spatially scanning the electron and heating pulses.

Similarly, we studied surface and bulk crystals of silicon, with and without adsorbates. Frame referencing to the ground-state structure shows the changes in the structure caused by the initiating pulse, from ground-state pattern at negative time to the observed change at positive time (Figure 12). The structural change is evident in the shift with time of the in-phase Bragg peak of the rocking curve, whereas the increase in vibrational amplitude is reflected in the broadening. The evolution takes place as a rise to a maximum shift and then a decay to the coordinates of the original structure. By gating on a Bragg spot, we followed the changes with time. As with GaAs, we observed the motion of surface and bulk atoms and their timescales (39). Following the femtosecond rise in electron temperature, electron-phonon coupling results in the population of optical phonons, which then generate, after picoseconds delay, acoustic waves (lattice expansion and compression), and finally lattice heating. Such a two-temperature description of heating is well known. Using UEC, we now can observe the ultrafast surface and bulk structural dynamics and follow the restructuring and diffusion at longer times.

Because we can vary the fluence of the initiating pulse, we also studied the structural changes involved in phase transitions when the temperature of the lattice is sufficiently high to cause large amplitude disorder. Initiating an ultrashort temperature jump of the amorphous structure with the infrared femtosecond pulse gives new diffraction ring patterns, which we followed as a function of time by referencing to the ground-state frame (Figure 12). The structural change is a phase transition to the liquid-like state (39).

Interfacial Water: Hydrophilic and Hydrophobic Substrates

The directional molecular features of hydrogen bonding and the different structures possible, from amorphous to crystalline, make the interfacial collective assembly of water, on the mesoscopic scale, much less understood. Structurally, the nature of water on a substrate is determined by forces of orientation at the interface and by the net charge density, which establishes the hydrophilic or hydrophobic character of the substrate. However, the transformation from ordered to disordered structure and their coexistence critically depends on the timescales for the movements of atoms locally and at long range. Therefore, it is essential to elucidate the nature of these structures and the timescales for their equilibration.

In a recent publication by Ruan et al. (64), we reported UEC determination of the structural dynamics of interfacial water following substrate infrared temperature jump. Interfacial water was formed on a hydrophilic surface (silicon, chlorine-terminated) or hydrophobic surface (silicon, hydrogen-terminated) under controlled UHV conditions. We identified the interfacial and ordered (crystalline)

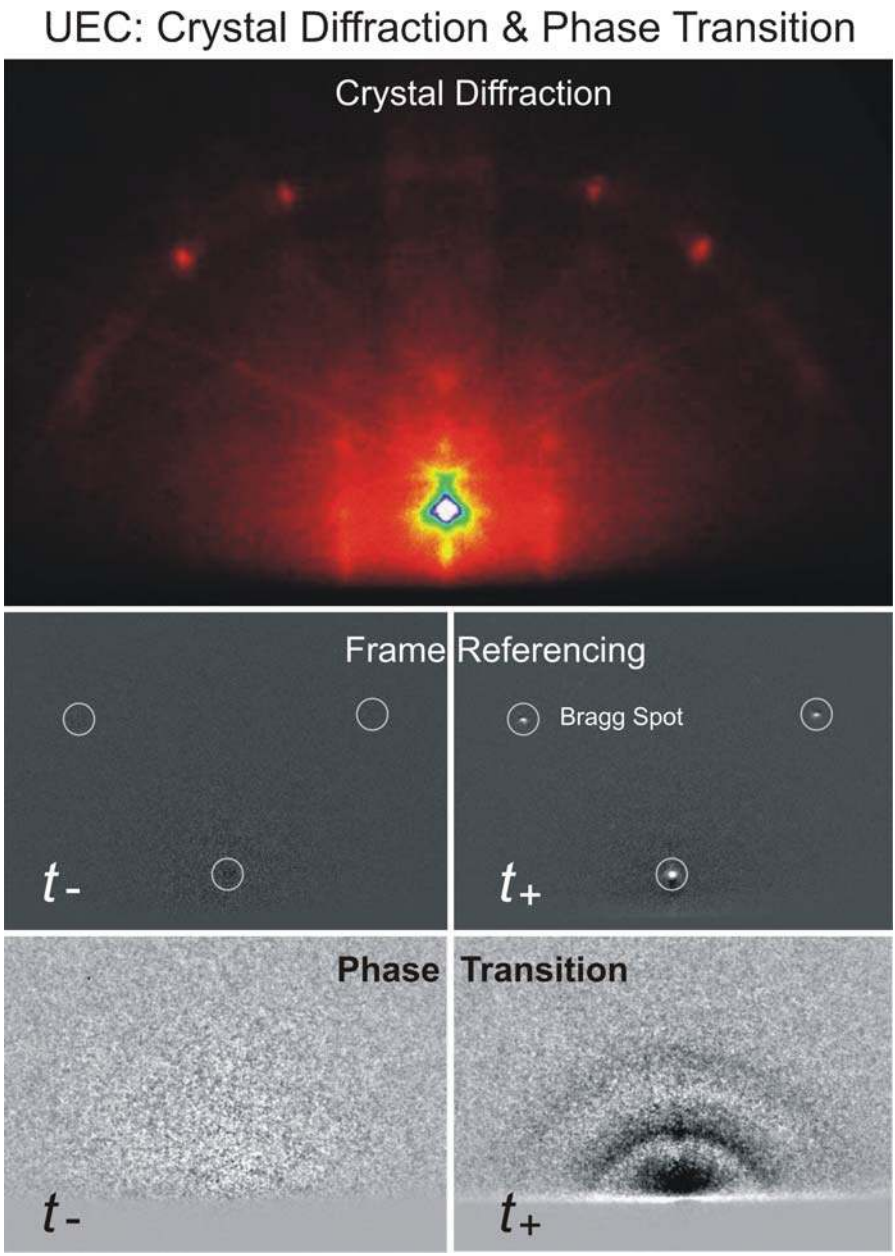

Figure 12 Ultrafast electron crystallography of single-crystal silicon surfaces and nanometer crystals. The evolution of structures, using frame referencing, and the phase transition at higher temperatures (diffraction rings) are displayed.

structure from the Bragg diffraction and the layered and disordered (polycrystalline) structure from the Debye-Scherrer rings (Figures 13 and 14). The temporal evolution of interfacial water and layered ice after the temperature jump was studied with monolayer sensitivity.

On the hydrophilic surface substrate the structure is cubic (I_c), not hexagonal (I_h), and structural dynamics are distinctive. The timescale for the breakage (large-amplitude motion) of long-range order of the interfacial layer (37 ps) is an order of magnitude longer than that for breaking hydrogen bonds in bulk liquid water, and the local OH · · O and O · · · O bond distances from diffraction are directly involved in the change but on different timescales. These results also indicate that the timescale for energy flow (in the 1 ps range) in the assembled water structure is much shorter than that of energy localization for desorption of individual molecules. Moreover, the restructuring time involving long-range order is longer than the time for amorphization, a process in which the O · · · O correlation is lost before the OH · · O correlation, defining the vibrational motion involved. Finally, there is the relevance to biological water—perhaps it is not accidental that the timescale for losing the hydrogen bond network (37 ps) is similar to that reported for interfacial water near hydrophilic protein surfaces (20 ps to 50 ps) and is very different from that of bulk water (700 fs to 1.5 ps); see Figure 3 and Reference 17 (and references therein).

On the hydrophobic surface, the structure is still cubic, but very different in order. The structural dynamics is also different. The interface is dominated by polycrystalline I_c, but coexisting in this phase are crystallite structures, not adjacent to the surface of the substrate; see Figure 14 for rings and spots diffraction, and the comparison with theory. The change in the structure of I_c has different temporal behaviors reflecting the distinct difference in the transfer of energy to polycrystalline and crystallite I_c. We note that for the hydrophilic substrate studied, water adjacent to the surface is crystalline, or nearly so, whereas that away from the surface is polycrystalline. These studies were made recently in this laboratory by D.-S. Yang, N. Gedik & S. Habershon, and a full account of these and the earlier study (64) will be published in a series of papers. The issues of interest are the coexistence of these structures, their different dynamics, and the timescales for energy transfer and disruption of the hydrogen bond network.

Bilayers of Crystalline 2D Fatty Acids: Molecular Assemblies

For the studies of membrane-type structures, we decided to first investigate a bilayer of fatty acids deposited on a hydrophobic surface substrate, invoking the well-known Langmuir-Blodgett (LB) technique. It allows for a controlled layer-by-layer deposition of ordered molecular films and has been used to create model biological membranes for studies under controlled conditions. Although biomembranes are more complicated by the presence of intercalaters, the LB bilayers represent the building blocks of lipid bilayers, in our case with the molecular chains extending up to ∼50 Å. LB films themselves are of considerable interest in

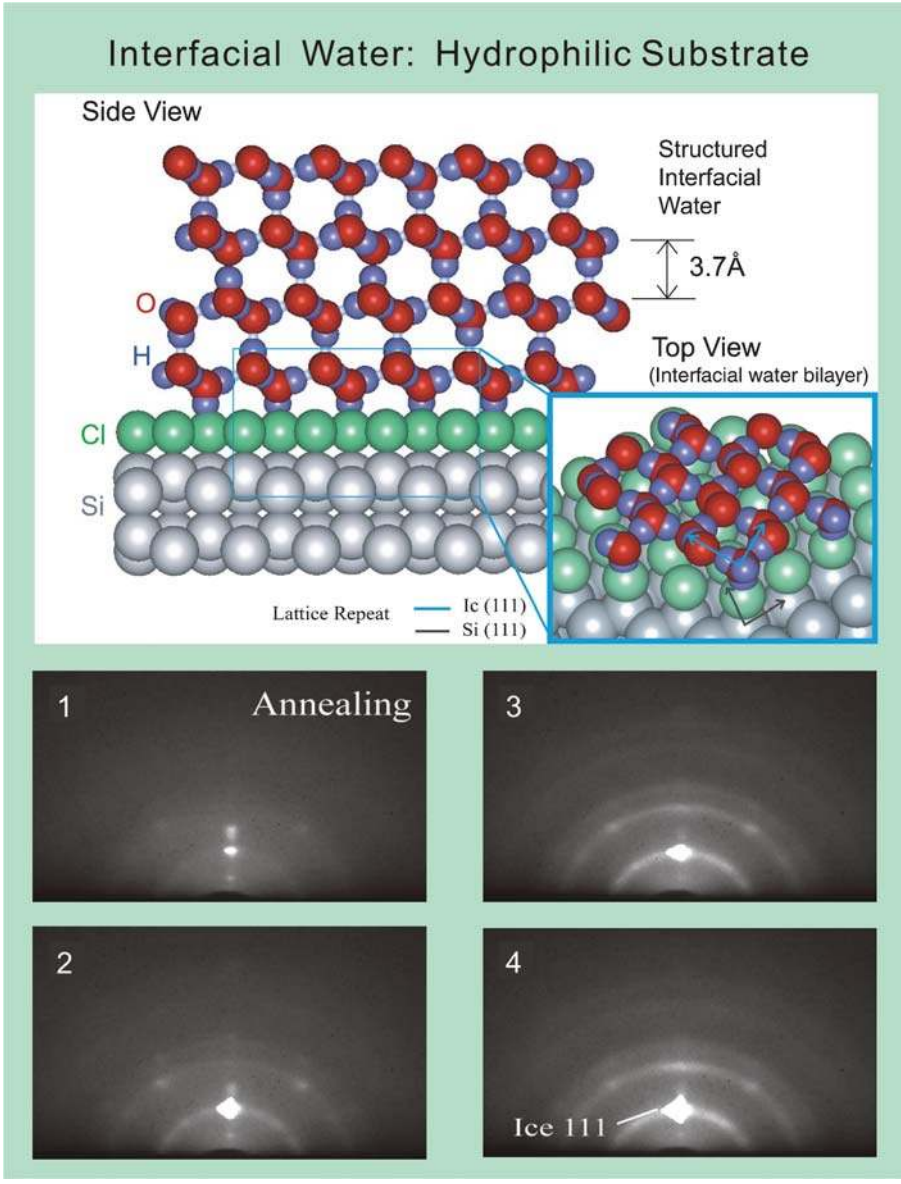

Figure 13 Ultrafast electron crystallography studies of interfacial water on a hydrophilic substrate. The coexistence of crystalline and polycrystalline structures (Bragg spots and Debye-Scherer rings) are clear in the patterns.

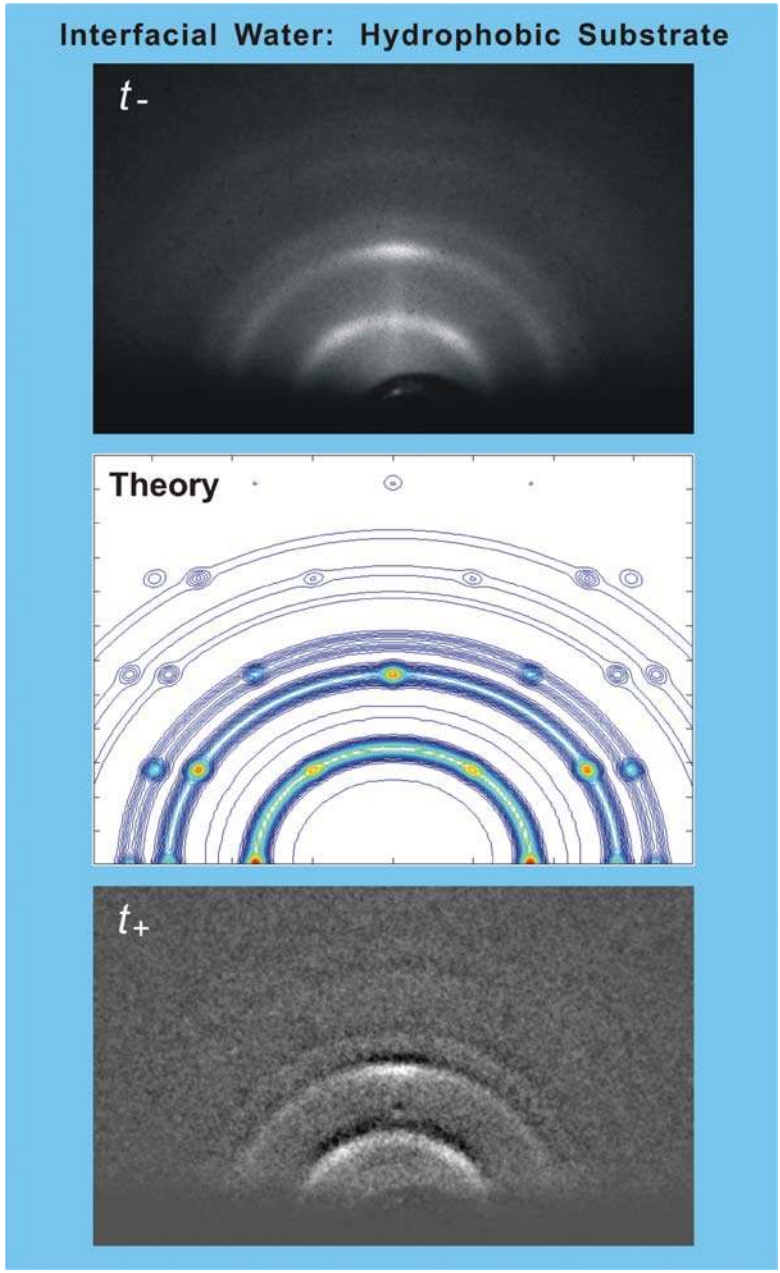

Figure 14 Ultrafast electron crystallography studies of interfacial water on a hydrophobic substrate. Shown also is the theoretical simulation of diffraction. (*Bottom*) Frame referencing at positive time to show the depletion of "old" structures and formation of "new" structures (*dark and white regions*).

various areas of research involving self-assembly, self-organization, and protein immobilization, and in technology developments such as molecular electronics and nonlinear optics.

Previous static diffraction studies have provided patterns and analyses with focus on the distances between the ions (X ray) and in thick films of many layers. In these investigations, however, the structures were not time-resolved and were not directly reflective of the influence of the supporting surface. Femtosecond time-resolved studies (65) of biomembranes have examined the spectroscopy of local probes, and time-resolved X-ray diffraction studies have shown the laser-induced disorder above the damage threshold of the organic film (66). In the former study the structure cannot be determined, and for the latter the film was 83 layers and it was not possible to solve for the structure of the fatty acid assembly. The laser-heating resulted in a destructive change above the damage threshold.

Recently, Chen et al. (67) reported on UEC of one bilayer (two chains of $C_{19}H_{39}COOH$) of arachidic (eicosanoic) fatty acid. With UEC sensitivity and resolution, we determined the structure, thus establishing the orientation of the aliphatic chains and obtaining the subunit cell molecular $–CH_2–CH_2–$ dimensions; Figure 15 displays the structure of the bilayer studied and the subunit cell in two directions. In the same publication we reported the observation of the coherent and anisotropic dynamical expansion in the bilayer structure and the restructuring toward equilibration at longer times. The timescales involved following the temperature jump were obtained from the diffraction frames taken every 1 ps (Figure 15). From these studies a structural dynamics picture emerges for the bilayer on the substrate and for its atomic motions.

All diffraction patterns are composed of spots (and/or streaks), showing the high quality of the 2D crystalline structure of the arachidic acid bilayer and the underlying hydrogen terminated Si(111) surface. The diffraction patterns at negative times and at low incidence angle of the electrons, parallel and perpendicular to the dipping direction, give the tilt angle of the chains (nearly zero) and provide the subunit cell parameters of the bilayer: $a_0 = 4.7$ Å, $b_0 = 8.0$ Å, and $c_0 = 2.54$ Å. The symmetry of the bilayer is an orthorhombic R(001) packing, with the (001) plane parallel to the Si(111) surface. At higher incidence angle, additional diffraction Bragg spots appear, resulting from the single crystal silicon substrate, which can easily be indexed (see above).

These experimental values for the lattice parameters within the plane differ from the predicted theoretical values of $a_0 = 4.96$ Å and $b_0 = 7.4$ Å (68). The difference can be explained by the fact that the theoretical values were calculated for infinite aliphatic chains and do not take into account the carboxylic end group of fatty acids. Moreover, the bilayer consists only of two monolayers, so the substrate and the deposition conditions (e.g., the dipping pressure or the pHs of the solution) all have an important role in the order at the interface. The spacing c_0 between CH_2 planes agrees very well with the theoretical value of 2.54 Å, as it represents separation between strong C–C bonds. The rocking curves, the changes of diffraction with incidence angle, were obtained and the

observations indicate a significant coherence length (nanometers) along the fatty acid chains.

With the frame-reference methodology invoked in these UEC studies, we obtained the structural dynamics selectively for the bilayer. As shown in Figure 15, immediately after the heating pulse (0 ps and 1 ps frames), an intensity loss of the Bragg spots is observed, as dark (*white*) spots evolve in the different frames. The

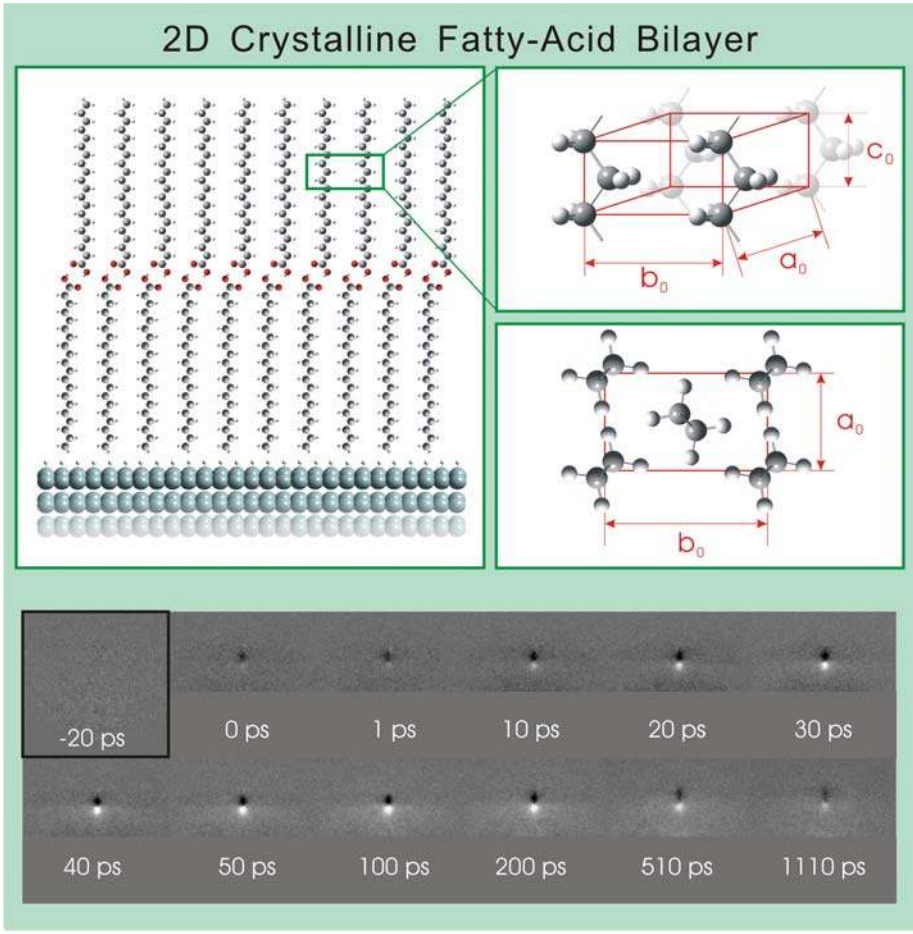

Figure 15 Ultrafast electron crystallography of 2D fatty-acid bilayers. Shown are the subunit cell structure determined and the dynamics from the frame referencing taken following the heat pulse to the substrate. The frames at 0 and 1 ps show the onset of structural changes, and the frames at longer times show the restructuring toward the equilibrium state.

change in the Bragg spots becomes more prominent over time (10–100 ps). The lower part of the peaks becomes brighter while the upper part becomes darker, showing a downward shift of the Bragg spots. At longer times, the patterns get fainter again, indicating that the peaks are moving back to their original position. Remarkably, both the heating and electron pulses, because of their timed repetition, ultrashort durations, and fluxes, do not damage the bilayer, as we repeated these experiments many times without observing damage.

In the vertical direction for all diffractions of the bilayer (c-component of the momentum transfer s-vector) we observe structural change. The behavior represents an initial expansion ($\Delta c_0 = 0.1$ Å) of the subcell in the bilayer after impulsive heating of the substrate followed by a subsequent contraction due to the heat dissipation. The expansion takes place with a time constant of 25 ps, whereas the subsequent compression occurs with 55 ps time constant, and the much longer time compression is a restructuring on the nanosecond timescale. Within our resolution, no significant change in lattice spacing is observed in the plane perpendicular to the molecular chains.

Structural dynamics of the bilayer can now be pictured. Because there is no absorption resonance for the fatty acids at the wavelength of the heating pulse, the pulse is absorbed only by the substrate and the bilayer is practically transparent. The heating is through the phonon temperature described above in our studies of Si and GaAs crystals (here substrate). Although the energy is directly transferred into the bilayer from the substrate, the expansion in the bilayer is significant along the aliphatic chains of the molecules, indicating an efficient and "wire-like" energy transfer within the fatty acid assembly. The covalent bondings in the chains, as opposed to the weak interactions across chains, facilitate such directional motion, besides the 2D stacking interaction in the crystal-like structure. This apparent nonequilibrium behavior must be handled cautiously.

At the maximum extension of the fatty acids the effective temperature is above the melting point of the assembly (in the range of 100°C), but the structure is far from equilibrium primarily in modes of the stretch and scissor (and twist) vibrations of the chains. Thus the motions along the chains should reflect the behavior of coupled oscillators—the forming of wave motion by local change in velocity and amplitude (or diffusion). If true, the behavior is that of a soliton-type motion. Molecular dynamics simulations (in collaboration with Professor T. Shoji's group) and theoretical modeling (Dr. J. Tang, this group) of anharmonically coupled bonds are works in progress to address the timescales involved, the nature of coherent structural dynamics, and the incoherent energy dissipation in the restructuring at long times. An anisotropic expansion of the bilayer may prove significant in explaining mechanisms of motion and transport, and for this reason we are also examining biological membranes. So far we have studied multiple-layered fatty acid systems and phospholipids and are continuing to explore the effect of layer thickness on diffraction changes, position, and intensity. There is another dimension to this work, namely the origin of self-assembly (69) and crystallization, and UEC is our method of choice for the reasons given above.

ULTRAFAST ELECTRON MICROSCOPY

Transmission electron microscopy (TEM) with its wide-ranging arsenal of tools has long been a powerful method in many areas of research, allowing for subnanometer spatial resolution but lacking the ultrashort time resolution. Optical microscopy, using fluorescent probes, e.g., green fluorescent proteins, has provided the means to visualize events occurring in vitro and within cells (41 and references therein). However, despite possessing the capability for temporal resolution, optical methods are limited in their spatial resolution to the wavelengths employed, typically 200–800 nm. The ultimate techniques would be those that have the spatial resolution of electron microscopy and the time resolution of optical methods. As mentioned above, the atomic length scale can be studied with diffraction, but for biological and nanoscopic materials with characteristic length scales ranging from nanometers to micrometers, electron microscopy enjoys unique advantages.

Lobastov et al. (41), in a recent publication, reported the development of 4D UEM, which provides the ability to image complex structures with the spatial resolution of TEM, but as snapshots captured with ultrafast electron packets derived from a train of femtosecond pulses. The images and diffraction patterns were obtained at 120 keV for materials (single crystals of gold, amorphous carbon, and polycrystalline aluminum) and for biological cells of rat intestines. The strobing packets contain on average one electron per pulse and the specimen dose is a few electrons per $Å^2$, but the pulses are now fully controlled in space and time.

Conceptually, we built on the machinery of UED and UEC, but with a fundamental difference, namely the realization of the significance of timed, single-electron pulses for imaging in UEM. The design of 4D UEM is shown in Figure 5, which outlines the interfacing of the femtosecond optical system with the transmission electron microscope. Space-charge broadening and defocusing of electron pulses and stability of the electron flux during imaging are major issues that we had to resolve. To circumvent space-charge-induced broadening and the concomitant decrease in the ability of the microscope optics to focus these electrons, we have redesigned the transmission electron microscope by directly illuminating the photocathode with extremely weak femtosecond pulses, but as a high-frequency train of pulses separated by nanosecond or longer intervals. This crucial advance empowered us to successfully record images and diffraction patterns with the required sensitivity and dosage, but with new dimensions.

The approach is entirely different from the one used in the important work of Dömer & Bostanjoglo (70 and references therein). They utilized a single giant pulse with $\sim 10^8$ electrons, and the pulses are photoelectrically generated as in UED and UEC. Their microscope utilizes a ~20 ns electron-pulse duration and a current of ~2 mA. Such pulses, which were used to study laser-induced melting in metals, pack within them the large number of electrons ($\sim 10^8$) that are detrimental to achieving ultrashort pulse imaging. Moreover, because the time window for imaging in those experiments is nanoseconds, the uncertainty in spatial resolution due to noise statistics is on the order of micrometers, as pointed out by Bostanjoglo

(71). In fact our attempt to use amplified femtosecond light pulses with much higher peak power density (on the order of 10^{12} W/cm^2) resulted in electron bunches that were impervious to focusing by the microscope optics, and no doubt much broader pulses due to electron-electron repulsion.

Using our 4D UEM we obtained images of materials, polycrystalline and single crystals (Figure 16). For calibration, we also obtained "images" when the femtosecond pulses entering the microscope were blocked. The fact that no images were observed when the light pulses were blocked indicates that the electrons

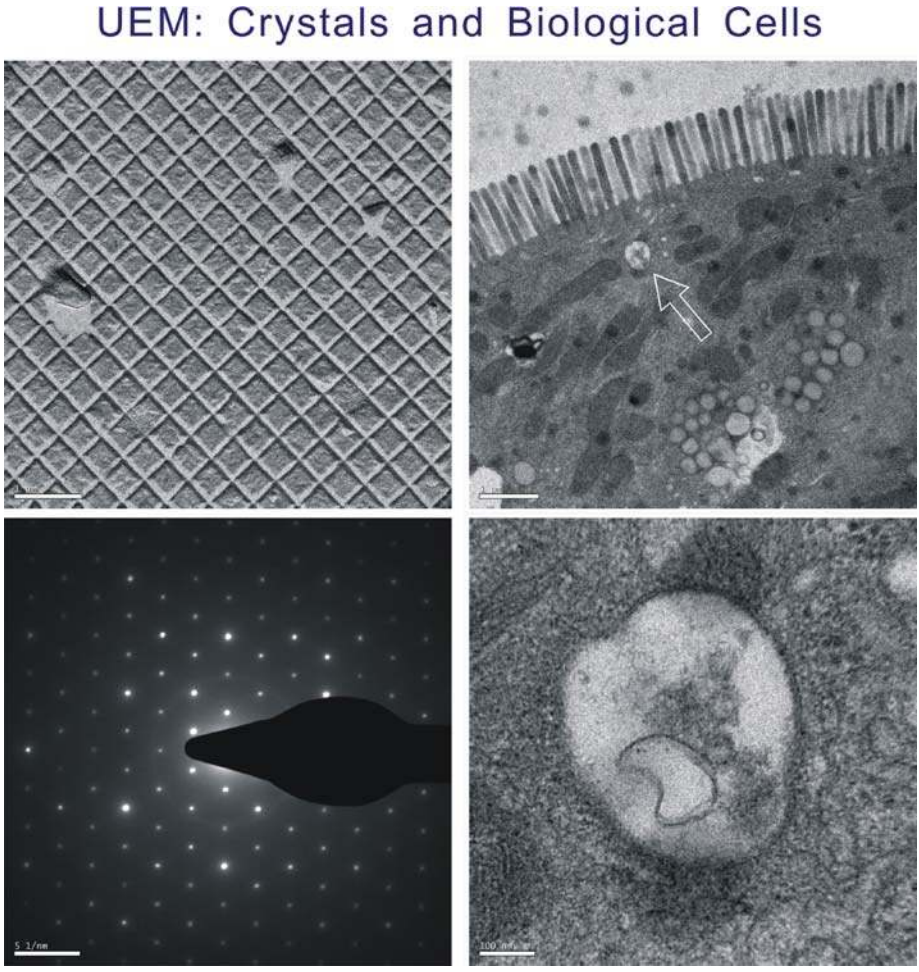

Figure 16 Ultrafast electron microscopy of biological cells from rat intestines at two magnifications (*top* and *bottom right*). Shown also are a typical image of gold crystals (*top*, *left*) and the diffraction pattern (*bottom*, *left*) (see text).

generated in the microscope were indeed those obtained optically and that thermal electrons were negligible. The microscope can operate in UEM and TEM modes, and for atomic-scale investigations, we operated UEM in the diffraction mode by adjusting the intermediate lens to select the back focal plane of the objective lens as its object (Figure 16). The novel attributes of UEM encouraged us to test the viability of imaging biological cells. UEM images of rat intestinal cells were obtained in a few seconds and both the microvilli as well as the subcellular vesicles of these epithelial cells were visualized in the UEM images. As in the case of UED and UEC, UEM is now poised for measurements of structural dynamics. For such time-resolved investigations, the time axis is defined by distance steps in the arrangement of Figure 5, noting that one micron of path difference corresponds to a frame separation of 3.3 fs. Applications are numerous.

CONCLUDING REMARKS

Because of limitations of space, it was not possible to cover all studies made using UED, UEC, and UEM. In this review, we only highlighted the concepts, developments, and, by way of prototypical examples, the myriad of possible applications. In order to reliably introduce the fourth dimension (time) into structural determination and imaging in different phases we had to develop, through five generations of table-top instruments, the conceptual framework and methodology needed to reach the atomic-scale spatiotemporal resolution and to cover both Fourier space (diffraction) and real space (microscopy). Our current resolutions are: spatial, picometer to nanometer (UED and UEC to UEM) and temporal, 1 picosecond (UED), 300 femtosecond (UEC, transmission), and less than or equal to 100 femtosecond (UEM, single electrons). Only with frame-referencing at different times could we reach as low as 1% for the sensitivity of change and temporally isolate the transient structures. For convenience, we list the subjects studied and publications from this laboratory in Table 1, covering nearly a decade of research.

In the same year (1991) we proposed UED as a method for structural dynamics, Thomas (72) wrote a "News and Views" piece entitled *Femtosecond Diffraction*. Toward the end of the piece he concluded with the following words: "If the experiment does indeed prove successful it will mark the dawn of an important new era. . . ." It took exactly a decade (2001), and the evolution from UED-1 to UED-3, to transform a dream into realization, from the exploration of the potential of the approach to the explosion of the applications in real experimental determination of isolated, transient molecular structures. The robustness of UED-3 made it possible to study a variety of systems, and here we discussed two classes, prototypical chemical reactions and excited-state dark structures that bifurcate through radiationless transitions. In this UED-3 laboratory, we are currently continuing studies of structures in reactions and of excited states. Also, using a new apparatus we plan to study structural dynamics of macromolecular systems with the aid of new theoretical formulation, including charge density maps (60), of diffraction from isolated proteins. Oriented reactions (73, 74) are also part of the new effort in UED.

In retrospect, what is remarkable about Thomas' piece was its broader vision for the significance of determining structures in the act of change irrespective of the phase they are in. Our development of UEC, in both reflection and transmission modes, was for the sole purpose of extending UED to the condensed phase. Because of long-range order, it was possible to study structural dynamics of nanometer-scale crystals, surfaces, and molecular assembles on substrates. Here, we discussed prototypical cases of surface-atom motion, surface phase transition, interfacial water on hydrophobic and hydrophilic substrates, and structural dynamics of bilayers of fatty acids on hydrophobic substrates. In 2004, Thomas overviewed (75) the significance of UEC, but equally important were his views on potential applications in heterogeneous catalysis (76). Currently, our group is involved in extensions of UEC to studies of materials using transmission diffraction and biological assemblies using reflection diffraction. Transmission offers a better time resolution because of geometrical constraints in reflection, and for both we plan further improvement of the frame resolution in time by using composite-phase shaped optical pulses (77).

From diffraction in Fourier space, both UED and UEC provide atomic-scale spatial resolution. An inversion to real space requires theoretical machinery and, for obtaining refined structures, dynamical theory may be invoked. So far we have obtained structures using kinematic theory, principally because of the high electron energy, the sample density, and the relatively low atomic number of atoms. Imaging in real space is the property of TEM. In 4D UEM, the sample sees timed single-electron packets, thus removing the detrimental space-charge effects of defocusing and broadening of pulses in imaging. Here, it was shown that such a microscope can be applied to studies of materials and biological cells. In the same microscope, we obtained diffraction with atomic-scale spatial resolution, again using timed, single-electron packets.

Thomas, who has been following the trajectory of developments since its naissance, and who is a pioneer in the applications of microscopy to materials science (76, 78), has written a highlight (79) describing the revolutionary aspect of 4D UEM and the prospects for branched applications. Harris & Thomas (80) explored some applications in domains of biological macromolecules and solid state chemistry. It did not escape our attention that 4D UEM should find applications in many fields, in particular in biological imaging. The new microscope allows facile operation in two modes—the UEM mode and the conventional TEM mode—offering a universal methodology for structural studies in space and time. Moreover, because UEM has been designed using femtosecond pulse trains from the oscillator alone, without the need for an ultrafast pulse amplifier, it has the added technological advantage of being beguilingly simple and easy to integrate. It may also prove unique (3) for limiting heat and blurring of images, and possibly radiation damage (9, 81), points under study in this laboratory. Currently, we have one complete system operating at 120 keV, and shortly there will be three 4D UEMs, including single-pulse recordings at a higher number of electrons but with picosecond resolution. Applications involving higher spatial resolutions and microscopy-based advances (82–84) include studies of cryo and life cell imaging.

TABLE 1 Different generations of UED, UEC, and UEM: developments, subjects, and references

	Subject	References
Concept	Femtosecond transition-state dynamics	34
	Structural femtochemistry: experimental methodology	35
UED-1	Ultrafast diffraction and molecular structure	36
	UED: velocity mismatch and temporal resolution in crossed-beam experiments	61
	UED: molecular structures and coherent dynamics	73
	UED: experimental time resolution and applications	56
UED-2	Clocking transient chemical changes by UED	37
	UED: structures in dissociation dynamics of $Fe(CO)_5$	42
	UED: determination of radical structure with picosecond time resolution	96
	UED and direct observation of transient structures in a chemical reaction	97
	Ultrafast gas-phase electron diffraction	98
	Conformations and barriers of haloethyl radicals (CH_2XCH_2, X = F, Cl, Br, I)	99
	UED of transient $[Fe(CO)_4]$: determination of molecular structure and reaction pathway	102
	UED of transient cyclopentadienyl radical: a dynamic pseudorotary structure	103
UED-3	Direct imaging of transient molecular structures with ultrafast diffraction	38
	CF_2XCF_2X and CF_2XCF_2 radicals (X = Cl, Br, I): ab initio and DFT studies and comparison with experiments	58
	Ultrafast diffraction of transient molecular structures in radiationless transitions	100
	Ultrafast diffraction and structural dynamics: the nature of complex molecules far from equilibrium	101
	UED and structural dynamics: transient intermediates in the elimination reaction of $C_2F_4I_2$	57
	UED: complex landscapes of molecular structures in thermal and light-mediated reactions	104
	Direct determination of hydrogen-bonded structures in resonant and tautomeric reactions using UED	105
	UED: structural dynamics of the elimination reaction of acetylacetone	106
	Dark structures in molecular radiationless transitions determined by ultrafast diffraction	59
	UED: dynamical structures on complex energy landscapes	60
	UED: oriented molecular structures in space and time	74
UEC	UEC: transient structures of molecules, surfaces, and phase transitions	39

(*Continued*)

TABLE 1 (*Continued*)

	Subject	References
	UEC of interfacial water	64
	UEC of surface structural dynamics with atomic-scale resolution	62
	Structures and dynamics of self-assembled surface monolayers observed by UEC	69
	Atomic-scale dynamical structures of fatty acid bilayers observed by UEC	67
UEM	Four-dimensional UEM	41
	Ultrafast photoelectron microscope	110
Reviews and views	UED: a new development for the 4D determination of transient molecular structures	4
	Pulse, pump and probe	107
	Structural chemistry, foreward	108
	UED shapes up	109
	Diffraction, crystallography and microscopy beyond three dimensions: structural dynamics in space and time	3
	UED: from the gas phase to the condensed phase with picosecond and femtosecond resolution	40
	Chemistry and biology in the new age	111
	Femtosecond diffraction	72
	UEC: the dawn of a new era	75
	A revolution in electron microscopy	79

Time-resolved X-ray spectroscopy and diffraction are developing in many laboratories (27 and references therein; 28–33, 85–88). Ultrafast X-ray diffraction is still advancing to achieve the reliability and sensitivity required for experimental studies of molecular-scale phenomena; demonstrations in melting and phonon's coherence studies have been the prime examples. Pulsed X-ray sources can currently be produced from a synchrotron facility (pulse duration 30–100 ps), laser plasma generation (several 100 fs), high-harmonic (XUV) generation (hundreds of femtoseconds to hundreds of attoseconds), or the proposed free-electron laser. The issues involved are the brightness of the source, stability and detection sensitivity, and the wavelength to reach diffraction. Recently, multidimensional spectroscopy (89–92) was advanced to correlate frequencies of optical transitions with the temporal evolution, in analogy with NMR, thereby probing structural changes. Although structures are not resolved with atomic resolution it is possible with the aid of electronic structure calculations to elucidate ultrafast couplings and molecular changes in optical space. Electron dynamical changes are now becoming feasible to probe directly with spectroscopy on the subfemtosecond (attosecond) timescale (93 and references therein; 94, 95).

Four-dimensional UED, UEC, and UEM are at a turning point for exploitation in applications in physics, chemistry, and biology. The major hurdle in the use

of electron diffraction and imaging in microscopy was the space-charge problem, and with single-electron coherent packets, this problem no longer exists. Moreover, local structures of less than 10^5 unit cells, as opposed to an average over 10^{15} unit cells, can be explored and their constituents imaged in real space. In our laboratory, the applications span both the physical and biological sciences. In 1937, Davisson & Thomson received the Nobel Prize in physics "for their experimental discovery of the diffraction of electrons by crystals." That discovery was for "static" diffraction. Only 70 years later could the fourth dimension of time be introduced to diffraction and microscopy, integrating the physics of space and time in structural dynamics.

ACKNOWLEDGMENTS

This paper is based on a series of lectures (Cavendish's Scott Lectures) I gave in Cambridge, UK, in the spring of 2005. We gratefully acknowledge the generous support by the National Science Foundation for building the new generations of UED and UEC, and Caltech for some of the initial help in building UEM. Partial support was provided by the Air Force Office of Scientific Research for studies in UED. I thank all members of the "diffraction group," both present and past, and whose efforts, expressed in the publications cited, made the story told here possible; some parts are adapted from the original references. Originally, the vision for this new field met very noticeable resistance, but it was their dedication and hard work that made us sail through. For this review, I especially thank Spencer Baskin and Dmitry Shorokhov for their thorough reading of the manuscript and helpful comments, Jerry (Ding-Shyue) Yang for his help in the preparation of the figures, and De Ann Lewis for typing the manuscript uninterruptedly and late after work hours. Finally, I am grateful for the timely support granted by the Gordon and Betty Moore Foundation for the UST Center devoted to the new horizons of ultrafast microscopy in physics, chemistry, and biology.

LITERATURE CITED

1. McMillan PF, Clary DC, eds. 2005. *Philos. Trans. R. Soc. A* (Special Issue) 363: 309
2. Zewail AH. 2000. In *Les Prix Nobel: The Nobel Prizes 1999*, ed. T Frängsmyr, p. 103. Stockholm: Almqvist, Wiksell
3. Zewail AH. 2005. *Philos. Trans. R. Soc. A* 364:315
4. Srinivasan R, Lobastov VA, Ruan C-Y, Zewail AH. 2003. *Helv. Chim. Acta* 86: 1763
5. Zewail AH, ed. 1992. *The Chemical Bond: Structure and Dynamics.* Boston, MA: Academic
6. Henderson R, Unwin PNT. 1975. *Nature* 257:28
7. Deisenhofer J, Epp O, Miki K, Huber R, Michel H. 1985. *Nature* 318:618

8. Doyle DA, Cabral JM, Pfuetzner RA, Kuo AL, Gulbis JM, et al. 1998. *Science* 280:69
8a. Bass RB, Strop P, Barclay M, Rees DC. 2002. *Science* 298:1582
9. Henderson R. 1995. *Q. Rev. Biophys.* 28:171
10. Steiger B, Baskin JS, Anson FC, Zewail AH. 2000. *Angew. Chem. Int. Ed.* 39:257
11. Zou S, Baskin JS, Zewail AH. 2002. *Proc. Natl. Acad. Sci. USA* 99:9625
12. Wang Y, Baskin JS, Xia T, Zewail AH. 2004. *Proc. Natl. Acad. Sci. USA* 101: 18000
13. Xia T, Becker H-C, Wan C, Frankel A, Roberts RW, Zewail AH. 2003. *Proc. Natl. Acad. Sci. USA* 100:8119
14. Xia T, Wan C, Roberts R, Zewail AH. 2005. *Proc. Natl. Acad. Sci. USA.* 102:13013
15. Wan C, Fiebig T, Kelley SO, Treadway CR, Barton JK, Zewail AH. 1999. *Proc. Natl. Acad. Sci. USA* 96:6014
16. O'Neill MA, Becker H-C, Wan C, Barton JK, Zewail AH. 2003. *Angew. Chem. Int. Ed.* 42:5896
17. Pal SK, Zewail AH. 2004. *Chem. Rev.* 104:2099
18. Kamal JKA, Xia T, Pal SK, Zhao L, Zewail AH. 2004. *Chem. Phys. Lett.* 387:209
19. Zewail AH. 2001. *Nature* 412:279
20. Zewail AH. 2001. *Angew. Chem. Int. Ed.* 40:4371
21. Mark H, Wierl R. 1930. *Naturwissenschaften* 18:205
22. Davisson C, Germer LH. 1927. *Phys. Rev.* 30:705
23. Thomson GP, Reid A. 1927. *Nature* 119: 890
24. Pauling L, Brockway LO. 1935. *J. Am. Chem. Soc.* 57:2684
24a. Brockway LO. 1936. *Rev. Mod. Phys.* 8: 231
25. Hargittai I, Hargittai M, eds. 1988. *Stereochemical Applications of Gas-Phase Electron Diffraction*. New York: VCH
26. Goodman P, ed. 1981. *Fifty Years of Electron Diffraction.* Dordrecht: Reidel
27. Bressler C, Chergui M. 2004. *Chem. Rev.* 104:1781
28. Rousse A, Rischel C, Gauthier J-C. 2001. *Rev. Mod. Phys.* 73:17
29. Chin AH, Schoenlein RW, Glover TE, Balling P, Leemans WP, Shank CV. 1999. *Phys. Rev. Lett.* 83:336
30. Lindenberg AM, Kang I, Johnson SL, Missala T, Heimann PA, et al. 2000. *Phys. Rev. Lett.* 84:111
31. von der Linde D. 2003. *Science* 302:1345
31a. Sokolowski-Tinten K, Blome C, Blums J, Cavalleri A, Dietrich C, et al. 2003. *Nature* 422:287
32. Oulianov DA, Tomov IV, Dvornikov AS, Rentzepis PM. 2002. *Proc. Natl. Acad. Sci. USA* 99:12556
33. Ráksi F, Wilson KR, Jiang Z, Ikhlef A, Côté CY, Kieffer J-C. 1996. *J. Chem. Phys.* 104:6066
34. Zewail AH. 1991. *Faraday Discuss. Chem. Soc.* 91:207
35. Williamson JC, Zewail AH. 1991. *Proc. Natl. Acad. Sci. USA* 88:5021
36. Williamson JC, Dantus M, Kim SB, Zewail AH. 1992. *Chem. Phys. Lett.* 196:529
37. Williamson JC, Cao J, Ihee H, Frey H, Zewail AH. 1997. *Nature* 386:159
38. Ihee H, Lobastov VA, Gomez UM, Goodson BM, Srinivasan R, et al. 2001. *Science* 291:458
39. Ruan C-Y, Vigliotti F, Lobastov VA, Chen S, Zewail AH. 2004. *Proc. Natl. Acad. Sci. USA* 101:1123
40. Lobastov VA, Srinivasan R, Vigliotti F, Ruan C-Y, Feenstra JS, et al. 2004. In *Ultrafast Optics IV, Springer Series in Optical Sciences*, ed. F Krausz, G Korn, P Corkum, IA Walmsley, 95:419. New York: Springer; work was presented at the conference in Vienna (2003)
41. Lobastov VA, Srinivasan R, Zewail AH. 2005. *Proc. Natl. Acad. Sci. USA* 102: 7069
42. Ihee H, Cao J, Zewail AH. 1997. *Chem. Phys. Lett.* 281:10
43. Rood AP, Milledge J. 1984. *J. Chem. Soc. Faraday Trans. 2* 80:1145

44. Ischenko AA, Golubkov VV, Spiridonov VP, Zgurskii AV, Akhmanov AS, et al. 1983. *Appl. Phys. B* 32:161
45. Mastryukov VS. 1991. *Moscow Univ. Chem. Bull.* 46:30; Transl. *Vestn. Mosk. Univ. Ser. 2 Khimiya* 32:249 (In Russian)
46. Bartell LS, Dibble TS. 1990. *J. Am. Chem. Soc.* 112:890
47. Ewbank JD, Faust WL, Luo JY, English JT, Monts DL, et al. 1992. *Rev. Sci. Instrum.* 63:3352

47a. Lobastov VA, Ewbank JD, Schäfer L, Ischenko AA. 1998. *Rev. Sci. Instrum.* 69:2633

48. Ischenko AA, Schäfer L, Luo JY, Ewbank JD. 1994. *J. Phys. Chem*. 98:8673
49. Dudek RC, Weber PM. 2001. *J. Phys. Chem. A* 105:4167
50. Mourou G, Williamson S. 1982. *Appl. Phys. Lett.* 41:44
51. Williamson S, Mourou G, Li JCM. 1984. *Phys. Rev. Lett.* 52:2364
52. Elsayed-Ali HE, Mourou GA. 1988. *Appl. Phys. Lett.* 52:103
53. Aeschlimann M, Hull E, Cao J, Schmuttenmaer CA, Jahn LG, et al. 1995. *Rev. Sci. Instrum.* 66:1000
54. Cao J, Hao Z, Park H, Tao C, Kau D, Blaszczyk L. 2003. *Appl. Phys. Lett.* 83: 1044
55. Siwick BJ, Dwyer JR, Jordan RE, Miller RJD. 2003. *Science* 302:1382
56. Dantus M, Kim SB, Williamson JC, Zewail AH. 1994. *J. Phys. Chem.* 98:2782
57. Ihee H, Goodson BM, Srinivasan R, Lobastov VA, Zewail AH. 2002. *J. Phys. Chem. A* 106:4087; for the initial report, see Reference 38
58. Ihee H, Kua J, Goddard WA III, Zewail AH. 2001. *J. Phys. Chem. A* 105:3623
59. Srinivasan R, Feenstra JS, Park ST, Xu S, Zewail AH. 2005. *Science* 307:558
60. Shorokhov D, Park ST, Zewail AH. 2005. *Chem. Phys. Chem.* 6:2228
61. Williamson JC, Zewail AH. 1993. *Chem. Phys. Lett.* 209:10
62. Vigliotti F, Chen S, Ruan C-Y, Lobastov VA, Zewail AH. 2004. *Angew. Chem. Int. Ed.* 43:2705
63. Sundaram SK, Mazur E. 2002. *Nat. Mater.* 1:217
64. Ruan C-Y, Lobastov VA, Vigliotti F, Chen S, Zewail AH. 2004. *Science* 304:80
65. Bürsing H, Ouw D, Kundu S, Vöhringer P. 2001. *Phys. Chem. Chem. Phys.* 3:2378
66. Rousse A, Rischel C, Uschmann I, Förster E, Albouy PA, et al. 1999. *J. Appl. Cryst.* 32:977
67. Chen S, Seidel MT, Zewail AH. 2005. *Proc. Natl. Acad. Sci. USA* 102:8854
68. Kitaigorodskii AI. 1961. *Organic Chemical Crystallography.* New York: Consult. Bur.
69. Ruan C-Y, Yang D-S, Zewail AH. 2004. *J. Am. Chem. Soc.* 126:12797
70. Dömer H, Bostanjoglo O. 2003. *Rev. Sci. Instrum.* 74:4369
71. Bostanjoglo O. 2002. *Adv. Imaging Electron Phys.* 121:1
72. Thomas JM. 1991. *Nature* 351:694
73. Williamson JC, Zewail AH. 1994. *J. Phys. Chem.* 98:2766
74. Baskin JS, Zewail AH. 2005. *Chem. Phys. Chem.* 6:2261
75. Thomas JM. 2004. *Angew. Chem. Int. Ed.* 43:2606
76. Thomas JM, Thomas JW. 1997. *Principles and Practice of Heterogeneous Catalysis*. New York: VCH
77. Warren WS, Zewail AH. 1983. *J. Chem. Phys.* 78:2279, 2298
78. Thomas JM, Midgley PA. 2004. *Chem. Commun.* 2004:1253
79. Thomas JM. 2005. *Angew. Chem. Int. Ed.* 44:5563
80. Harris KDM, Thomas JM. 2005. *Crystal Growth and Design* (Special Issue). 5:2124
81. Glaeser RM. 1999. *J. Struct. Biol.* 128:3
82. Spence JCH. 1999. *Mater. Sci. Eng. Rep.* 26:1
83. Thomas JM, Terasaki O, Gai PL, Zhou WZ, Gonzalez-Calbet J. 2001. *Acc. Chem. Res.* 34:583

84. Howie A. 2004. *Microsc. Microanal.* 10: 685
85. Chen LX. 2005. *Annu. Rev. Phys. Chem.* 56:221
86. Moffatt K. 2003. *Faraday Discuss.* 122: 65
87. Plech A, Wulff M, Bratos S, Mirloup F, Vuilleumier R, et al. 2004. *Phys. Rev. Lett.* 92:125505
88. Nugent-Glandorf L, Scheer M, Samuels DA, Bierbaum V, Leone SR. 2002. *Rev. Sci. Instrum.* 73:1875
89. Mukamel S. 1995. *Principles of Nonlinear Optical Spectroscopy.* New York: Oxford Univ. Press
90. Zanni MT, Hochstrasser RM. 2001. *Curr. Opin. Struct. Biol.* 11:516
91. Jonas DM. 2003. *Annu. Rev. Phys. Chem.* 54:425
92. Brixner T, Stenger J, Vaswani HM, Cho M, Blankenship RE, Fleming GR. 2005. *Nature* 434:625
93. Drescher M, Krausz F. 2005. *J. Phys. B* 38:S727
94. Drescher M, Hentschel M, Kienberger R, Tempea G, Spielmann C, et al. 2001. *Science* 291:1923
95. Föhlisch A, Feulner P, Hennies F, Fink A, Menzel D, et al. 2005. *Nature* 436: 373
96. Cao J, Ihee H, Zewail AH. 1998. *Chem. Phys. Lett.* 290:1
97. Cao J, Ihee H, Zewail AH. 1999. *Proc. Natl. Acad. Sci. USA* 96:338
98. Williamson JC. 1998. *Ultrafast gas-phase electron diffraction.* PhD thesis. Calif. Inst. Technol., Pasadena, CA
99. Ihee H, Zewail AH, Goddard WA III. 1999. *J. Phys. Chem. A* 103:6638
100. Lobastov VA, Srinivasan R, Goodson BM, Ruan C-Y, Feenstra JS, Zewail AH. 2001. *J. Phys. Chem. A* 105:11159
101. Ruan C-Y, Lobastov VA, Srinivasan R, Goodson BM, Ihee H, Zewail AH. 2001. *Proc. Natl. Acad. Sci. USA* 98:7117
102. Ihee H, Cao J, Zewail AH. 2001. *Angew. Chem. Int. Ed.* 40:1532
103. Ihee H, Feenstra JS, Cao J, Zewail AH. 2002. *Chem. Phys. Lett.* 353:325
104. Goodson BM, Ruan C-Y, Lobastov VA, Srinivasan R, Zewail AH. 2003. *Chem. Phys. Lett.* 374:417
105. Srinivasan R, Feenstra JS, Park ST, Xu SJ, Zewail AH. 2004. *J. Am. Chem. Soc.* 126:2266
106. Xu SJ, Park ST, Feenstra JS, Srinivasan R, Zewail AH. 2004. *J. Phys. Chem. A* 108:6650
107. Hoffmann R. 1999. *Am. Sci*. 87:308
108. Karle J. 2000. *Struct. Chem.* 11:91
109. Helliwell JR. 2001. *Phys. World* 14:25
110. Lobastov VA, Zewail AH. 2004. U.S. Patent (pending)
111. Hall N. 2002. *Chem. Commun.* 2002:2185
112. Feenstra JS, Park ST, Zewail AH. 2005. *J. Chem. Phys.* 123:221104–1
113. Habershon S, Zewail AH. 2006. Development of genetic algorithm for determining molecular structures and conformations. *Chem. Phys. Chem.* In press
114. Lin MM, Shorokhov D, Zewail AH. 2006. Helicity resonance in UED of helix-to-coil transitions in proteins. *Chem. Phys. Lett.* In press

NOTE ADDED IN PROOF

Since the submission of this review, several relevant contributions have been made. These include References 112–114.

Annual Review of Physical Chemistry
Volume 57, 2006

CONTENTS